Spring 2019

Role of P-Glycoprotein in Alzheimer's Disease for Enhanced Brain Elimination of Amyloid-β

Hope Holt

ROLE OF P-GLYCOPROTEIN IN ALZHEIMER'S DISEASE FOR ENHANCED BRAIN ELIMINATION OF AMYLOID-β

by

Hope Holt

Bachelor of Science
Tennessee Technological University, 2007

Submitted in Partial Fulfillment of the Requirements

For the Degree of Doctor of Philosophy in

Biomedical Engineering

College of Engineering and Computing

University of South Carolina

2019

Accepted by:

Melissa A. Moss, Major Professor

Maksymilian Chruszcz, Committee Member

Chandrashekhar Patel, Committee Member

Mark Uline, Committee Member

Cheryl L. Addy, Vice Provost and Dean of the Graduate School

ACKNOWLEDGEMENTS

First and foremost, I would like to thank my husband, Wes, for all of his love, support, and understanding over the years. I would not have been able to do this without him. I would also like to thank my parents, family, and friends for being there for me, especially my nephews, Roman and Sebastian, always ready to play and have deep conversations about dinosaurs. I would like to thank Dr. Mark Uline, Dr. Shekhar Patel, Dr. Maks Chruszcz, and Dr. Abdel Bayoumi for the advice and mentorship they gave me, both on my research project and my future career. I am truly thankful for the lab members who came before me, Dr. Kayla Pate, Dr. Shelby Chastain, and Dr. Zebulon Vance who in addition to training me in the lab, became my dear friends. Also, I would like to acknowledge Dr. Nick Boltin, Dr. William Torres, and Michael Hendley, we started this BMEN graduate school journey together years ago and it would have been a much more boring experience without your friendships. To all of the undergraduate and high school students I have had the opportunity to work with, Elizabeth, Maddie, Julia, Ishawn, Brittany, Amber, Esha, Sonja, and Alessio, thank you. Finally, I would like to thank my advisor, Dr. Melissa Moss, for her excellent guidance and continued support as well as current and former lab members for their help.

ABSTRACT

Alzheimer's disease (AD), the most common form of neurodegenerative disorder, is characterized by deposition of amyloid-β (Aβ) plaques in the brain. Aβ monomer undergoes nucleation to form oligomers, then soluble aggregates, then fibrils which make up the plaques. Aβ oligomer species are believed to be the most neurotoxic aggregate species. Currently under investigation is a mechanism for Aβ removal from the brain, across the blood-brain barrier (BBB). P-glycoprotein (P-gp) is a membrane-bound efflux protein located on the apical, or blood, side of the BBB, which transports a wide variety of substrates. Further complicating this potential clearance mechanism is the reduction of P-gp cell surface expression in arteries exhibiting cerebral amyloid angiopathy (CAA), or the buildup of amyloid plaques around the arteries.

P-gp has been suggested as a potential Aβ clearance mechanism based on its ability to transport a wide variety of amphipathic substrates even though experimental evidence of Aβ transport via P-gp has been disputed. This study sought to examine and characterize Aβ aggregate species interaction with P-gp. Additionally, the potential deleterious relationship between P-gp and extended Aβ presence was investigated.

Of the four different Aβ aggregate species tested, monomer, oligomer, sonicated fibril, and fibril, only the Aβ oligomer demonstrated the ability to bind to P-gp. These Aβ oligomers displayed a selective interaction with the R-binding site, and not the H-binding site. However, this binding and interaction could not be confirmed in a cellular transport assay.

Extended Aβ aggregate species treatment at the apical surface of a cellular monolayer revealed no change in either the cell surface expression of P-gp or the transport capabilities of P-gp. Interestingly, when a cellular monolayer was treated from the basolateral surface with Aβ aggregate species, the active P-gp driven net efflux decreased. These results support interactions between Aβ oligomers and P-gp and motivate further investigation of P-gp as a therapeutic clearance mechanism for Aβ.

TABLE OF CONTENTS

LIST OF FIGURES

LIST OF SYMBOLS

P_e	Permeability coefficient
$\frac{dC}{dt}$	Rate of appearance of a substrate in the receptor chamber
V	Volume of receptor chamber
C_0	Initial substrate concentration in the donor chamber
A	Surface area of the membrane
$P_{e,\ B\rightarrow A}$	Permeability coefficient in the basolateral to apical direction
$P_{e,\ A\rightarrow B}$	Permeability coefficient in the apical to basolateral direction

LIST OF ABBREVIATIONS

Aβ.....amyloid-β protein

$A\beta_{1-40}$..... 40 amino acid isoform of amyloid-β protein

$A\beta_{1-42}$..... 42 amino acid isoform of amyloid-β protein

ABC ..... ATPase binding cassette

AD..... Alzheimer's disease

ADP.....adenosine 5'-diphosphate

ANOVA .....analysis of variance

ATP ..... adenosine 5'-triphosphate

BBB..... blood-brain barrier

BSA.....bovine serum albumin

Caco-2 ..... human epithelial colorectal adenocarcinoma cells

CHRB30.....Chinese hamster ovary cells

CO_2.....carbon dioxide

DAPI ..... 4', 6-diamidino-2-phenylindole

DMEM .....Dulbecco's modified Eagle's medium

DMSO ..... dimethyl sulfoxide

DTT.....dithiothreitol

EGTA.....ethylene glycol-bis (β-aminoethyl ether)-N, N, N', N'-tetra acetic acid

ELISA ..... enzyme-linked immunosorbent assay

F MIX.....amyloid-β fibril mixture

FBS .....fetal bovine serum

FIB ..... amyloid-β fibril

FPLC ..... fast protein liquid chromatography

HBMVEC ..... human brain microvascular endothelial cells

HFIP 1, 1, 1, 3, 3, 3-hexafluoro-2-propanol

hMDR1-MAC ..... P-gp humanized mouse model

KCl ..... potassium chloride

LRP-1 ..... low-density lipoprotein receptor related protein 1

M ..... molar, SI unit for mol/L

MDCK ..... Madin Darby canine kidney cells

MDR1 ..... multidrug resistance protein 1

MgATP ..... magnesium adenosine 5'-triphosphate

MON ..... amyloid-β monomer

NaCl ..... sodium chloride

NaOH ..... sodium hydroxide

NaOV ..... sodium orthovanadate

OLIG ..... amyloid-β oligomer

p ..... p-value test statistic

P MIX ..... amyloid-β protofibril mixture

P-gp ..... P-glycoprotein

P_i ..... inorganic phosphate

SDS ..... sodium dodecyl sulfate

SE ..... standard error

SEC ..... size exclusion chromatography

TEER ..... transepithelial electrical resistance

ThT ..... thioflavin T

TRITC ..... tetramethyl rhodamine

VEH ..... vehicle

CHAPTER 1

BACKGROUND AND SIGNIFICANCE

1.1 Alzheimer's Disease

Every 65 s someone develops Alzheimer's disease (AD) in the US. Over 44 million people worldwide have been diagnosed with AD, making it the most common neurodegenerative disorder. As the population continues to age, these numbers are only expected to increase in the coming years. AD is already the sixth leading cause of death in the US. While the other top ten causes of death, including heart disease, cancer, HIV, and stroke, have dramatically reduced their mortality rate since the year 2000, deaths from AD have risen by 123%[1]. Additionally, AD is the only one of the top ten that is unable to be cured, prevented, or slowed.

In 1906, Dr. Alois Alzheimer described a neurodegenerative condition, now known as AD, which included symptoms of short-term memory loss and behavioral changes as well as the presence of amyloid plaques and neurofibrillary tangles[2,3]. These plaques, considered hallmarks of AD, are formed by the amyloid-β (Aβ) protein. Aβ monomer is commonly found throughout the body and is non-toxic. While the function of Aβ monomer is still under investigation, in the disease state, Aβ monomer nucleates to form oligomers, a neurotoxic Aβ aggregate species[4–15]. Aβ oligomers continue the aggregation process to form soluble intermediates, then Aβ fibrils, which make up the plaques[11,16–23]. While most therapeutic strategies target this aggregation pathway[18–20], this approach has not yet been

successful; additional novel therapeutic targets are needed and one such target mechanism is clearance[24–27].

1.2 Transport Across the Blood-brain Barrier

The blood-brain barrier (BBB) is the single endothelial cell thickness making up the capillary wall in the brain. While the capillary wall in other parts of the body is semi-discontinuous to allow for the free exchange of molecules, the capillary wall of the BBB is characterized by its tight junctions and high density of cells. These tight junctions require most transport into and out of the brain to be active transport via membrane-bound proteins[28–30].

P-glycoprotein (P-gp) is a membrane-bound efflux protein located on the apical side of the BBB, as well as in the intestine, liver, and kidneys[31–38]. P-gp, encoded by the multi-drug resistance 1 (MDR1) gene[39–43], evolved as a defense mechanism and transports a wide variety of substrates[44–47]. It is a member of the ATPase binding cassette (ABC) transport protein family, using energy obtained from the hydrolysis of ATP to transport substrates into the capillary for removal through the vasculature[48–55]. The structure of P-gp consists of two cassettes that share a 65% amino acid similarity. The N-terminal cassette contains six transmembrane domains, followed by an ATP binding site, connected to the C-terminal six transmembrane domains and ATP binding site[55–60].

Most P-gp substrates are amphipathic in nature and include many chemotherapeutic, immunosuppressive, and anti-inflammatory agents in addition to calcium channel blockers. Aromatic residues line the binding pockets, and it is thought the hydrophobic region of a substrate binds to P-gp[46,57,61–67]. There are two well described binding pockets, the H site and the R site, named for their fluorescent substrates[61,65,68–71].

The H-binding site binds and transports Hoechst 33342[57,61,68,72,73], while the R-binding site binds and transport Rhodamine 123[34,46,61,66,68,74–77]. When both sites are occupied, they can work cooperatively, increasing the transport rate for each substrate compared to the substrate's transport rate alone[65,68]. This cooperative binding could be exploited in the investigation of a potential therapeutic.

BBB *in vitro* models

Human brain microvascular endothelial cells (HBMVECs) are usually used to model the BBB *in vitro*[28,78–80]. They form tight junctions in the presence of hydrocortisone and grow easily into monolayers. However, it can be difficult to study P-gp in such a system due to P-gp's low relative expression. Additionally, there are brain microvasculature cell models from different species investigated alone or in co-culture to create a BBB model, which exhibit similar difficulties in studying P-gp specifically.

Two non-brain microvasculature cell-based models used to study P-gp include human epithelial colorectal adenocarcinoma (Caco-2) cells and Madin Darby canine kidney (MDCK) cells[37,81–84]. Over time, Caco-2 cells have been differentiated and polarized to mimic cells in the small intestine, exhibiting tight junctions and expressing transporter proteins such as P-gp. MDCK cells express a small amount of canine P-gp naturally. However, these cells serve as a parental line to the MDCK-MDR1 cell line, which has been transfected to overexpress human P-gp[85]. MDCK MDR1 cells have relatively high human P-gp expression compared to other cell types and also express tight junction proteins[85–89]. It has been demonstrated that both Caco-2 and MDCK-MDR1 cells are reliable models of the BBB when compared to rat brain microvasculature endothelial cells[82]. In this study, MDCK-MDR1 cells exhibited BBB properties, including tight

junction proteins and P-gp expression, in 3-4 days, while the Caco-2 cells displayed BBB properties in 19-21 days, and MDCK-MDR1 cells are more widely used in the literature as a BBB model[37,81–84,90–92].

1.3 Role of P-gp in AD

In 2004, a study of brain tissue obtained from non-demented elderly people showed a local inverse correlation of the expression of P-gp and the deposition of aggregated Aβ protein[93,94]. Vogelgesang *et al* correlated the level of P-gp expression with the level of Aβ aggregation and cerebral amyloid angiopathy, or the deposition of Aβ around small and mid-sized arteries. While the tissue samples all belonged to elderly subjects, the goal of this study was to investigate early AD markers and trends, so samples for late stage dementia patients were excluded. These findings insinuate P-gp may have an important role to play in the AD disease state.

Using inverted vesicles made from CHRB30 cells, Lam *et al* measured Aβ in its monomeric state as it was being transported across the plasma membrane[25]. These inverted vesicles, where P-gp is oriented towards the bulk solution, were in solution with ATP and either $A\beta_{1\text{-}40}$ or $A\beta_{1\text{-}42}$. Lam *et al* observed that the transport of either Aβ species across the membrane was dependent upon the presence of both ATP and P-gp showing that Aβ is a substrate of P-gp.

Moving to an in vitro model, Lam *et al* transfected cell lines that expressed varying levels of P-gp to overexpress Aβ. The cells with the highest expression of P-gp excreted the most Aβ. Wild type and P-gp knockout mice injected with both $A\beta_{1\text{-}40}$ and $A\beta_{1\text{-}42}$ showed increased clearance in the wild type mouse[95]. These studies and others suggest

that Aβ clearance from the brain into the blood could be diminished by a decrease in expression of P-gp at the BBB[95–100].

Kuhnke *et al* studied the mediation of Aβ transport by P-gp by using cells cultured in a monolayer to simulate the BBB[101]. Using fluorescently labelled $A\beta_{1\text{-}40}$ and $A\beta_{1\text{-}42}$, it was determined P-gp facilitates the removal of both species. Additionally, Kuhnke *et al* used a ThT fibrillogenesis assay to show the Aβ peptides transported across the cell monolayer were not in a fibrillar form but were mostly soluble aggregates. This shows that aggregated Aβ is also a substrate of P-gp.

1.4 Study Overview

Due to P-gp's ability to transport a wide variety of amphipathic and hydrophobic substrates, the most likely Aβ aggregate species able to be transported in Aβ oligomers. Aβ oligomers are slightly amphipathic with concentrated hydrophobic amino acids at the C-terminus. Aβ oligomers present a hydrophobic surface as evidenced by binding of hydrophobic dyes[20]. Aβ oligomers are the only Aβ aggregate state with the ability to enter the lipid bilayer, the preferred access to P-gp's binding sites[62,63]. This study investigated the hypothesis that P-gp preferentially binds and transports a specific Aβ aggregate state, oligomers, out of the brain. However, this clearance mechanism may be disrupted with the loss of P-gp in vessels containing cerebral amyloid angiopathy. Thus, this study additionally investigates the hypothesis that the presence of Aβ at the BBB can exasperate the disease state by reducing levels of P-gp available at the cell membrane for transport. To test these hypotheses, the binding and transport of Aβ by P-gp and the effect of Aβ on the presence of P-gp were examined separately. These studies comprise the two aims of this work and are described below.

1.4.1 Aim 1: To Demonstrate the Selective Binding and Transport of Aβ Oligomers via P-gp

The binding capability of Aβ by P-gp has been previously studied by a variety of groups; however, the effect of various aggregate species of Aβ have not been considered. This aim seeks to identify the Aβ aggregate species selectively binding to P-gp for transport and then characterize that binding relationship. First, experimentation compares the transport of Aβ aggregate species by P-gp across inverted P-gp membranes. Subsequently, those species with the highest transport are characterized for binding site interaction using MDCK-MDR1 cells by measuring the accumulation of a fluorescent substrate specific for each of P-gp's binding sites. P-gp has two well-described binding sites, the H-binding site, characterized for its binding of Hoechst 33342, and the R-binding site, characterized for its binding of Rhodamine 123. Finally, transport across monolayers formed by MDCK-MDR1 cells will be measured to assess the effect of Aβ aggregates on directional transport of Rhodamine 123. Comparing transport across these cell monolayers will quantify the role of P-gp in a biological system. The addition of alternative substrates with well described binding sites of P-gp to this assay allows further description of the binding relationship between Aβ and P-gp. These observations validate that P-gp is a viable target of potential AD therapeutics.

1.4.2 Aim 2: To Elucidate the Effect of Aβ Aggregate Species on P-gp Cell Surface Levels and Associated Transport

It has been shown that Aβ to P-gp binding can signal P-gp degradation in the cell[102]. This aim investigated the Aβ aggregate species responsible for this action using

MDCK-MDR1 cells to determine if the presence of Aβ aggregate species reduced the level of P-gp on the cell surface. Immunocytochemistry was used to quantify P-gp available at the cell membrane for transport, while cellular accumulation assays were used to verify the transport abilities of that P-gp. Additionally, cells were treated at the basolateral surface for a cellular transport assay to determine if the location of the Aβ treatment relative to the cell's polarity exposed any effect on the function of P-gp. These studies explore the deleterious effect of Aβ aggregate species on the availability of P-gp on the cell membrane. Fully describing the relationship between Aβ aggregate species and P-gp is necessary to appropriately target P-gp with a potential AD therapeutic.

1.5 Innovation

Almost 250 potential drugs for the treatment of AD were tested in clinical trials between 2002-2012(most recent data available). However, only one drug was successful, bringing the current total number of drugs approved by the FDA available in the US to five – Aricept, Razadyne, Namenda, Exelon, and Namzaric[1]. Additionally, instead of treating the underlying disease state, each is only able to improve the symptoms of AD temporarily.

Previous studies concerning potential therapeutics in AD have targeted the amyloidgenic aggregation pathway. These possible therapeutics have investigated a compound's ability to alter the Aβ aggregate's morphology and size to reduce the overall neurotoxicity. Unfortunately, while many of these compounds have been tested, most fail as drugs and have resulted in few clinical trials. This is hypothesized to result from the low specificity and affinity of the Aβ inhibitors. In this study, a novel therapeutic target is pursued by investigating an Aβ clearance mechanism. By targeting this pathway, the presence of Aβ in the brain will decrease, resulting in a decrease in aggregation due to the

process' nucleation dependency. This decrease in aggregation should lead to a reduction in neurotoxicity and a decrease in neurodegeneration. A comprehensive description of the relationship between P-gp and Aβ aggregates will highlight a pathway for Aβ clearance from the brain via transport across the BBB. In addition, as potential therapeutics would be acting on the BBB, instead of having to cross the BBB and act on the brain, the relevant bioavailability of a potential therapeutic will be higher.

CHAPTER 2

MATERIALS AND METHODS

2.1 Materials

$A\beta_{1-40}$ was purchased from Bachem (Torrence, CA) or AnaSpec, Inc. (San Jose, CA). $A\beta_{1-42}$ was obtained from AnaSpec, Inc. Thincert membranes and cell culture 6-well and 24-well plates were obtained from Grenier Bio-one (Kremsmünster, Austria). P-gp inverted vesicles and cell culture 96-well plates were purchased from Corning (Corning, NY). Anti-P-gp (P7965) was purchased from Millipore Sigma (Burlington, MA). Normal Donkey serum and Cy3 was purchased from Jackson Immunoresearch (West Grove, PA). Other chemicals were purchased from VWR (Radnor, PA).

2.2 Preparation of $A\beta_{1-40}$ Monomer

Lyophilized $A\beta_{1-40}$ was purified to obtain monomeric protein prior to use in experiments. Fast protein liquid chromatography (FPLC) that utilizes size exclusion chromatography (SEC) on a Superdex 75 HR 10/300 column (GE Healthcare, Piscataway, NJ, USA) was used to remove any seeds from which aggregates can grow. Prior to injection, $A\beta_{1-40}$ was reconstituted in 50 mM NaOH at 2 mg/mL to minimize the formation of small aggregates. The system was pretreated with 2 mg/mL BSA in order to aid in the reduction of nonspecific Aβ interaction with the column's dextran matrix. Protein elution occurred in 100 mM HEPES Tris buffer (pH 7.4). $A\beta_{1-40}$ monomer concentration was

calculated using the extinction coefficient of 1450 M^{-1} cm^{-1} at 276 nm[21] and Beer-Lambert law. Purified $A\beta_{1-40}$ monomer was used fresh in assays and for aggregation into $A\beta_{1-40}$ fibrils.

2.3 Preparation of $A\beta_{1-42}$ Oligomer

$A\beta_{1-42}$ was solubilized in cold HFIP at 4°C for 1 h. The solution was then aliquoted and the HFIP was allowed to evaporate overnight at 25°C. Protein films were stored at -80°C until use. Dried films of $A\beta_{1-42}$ were resuspended in DMSO at a concentration of 1.5 mM. For the in vitro assays, protein was diluted to 30 μM in 100 mM HEPES-Tris buffer (pH 7.4) containing 1 μM NaCl to initiate oligomerization. After 15 min, the reaction solution was diluted for use. For cellular based assays, protein was diluted to 15 μM in 12 mM phosphate buffer (pH 7.4) containing 1 μM NaCl. After 30 min, the reaction solution was diluted for use.

2.4 Preparation of $A\beta_{1-40}$ Fibril

SEC-purified $A\beta_{1-40}$ monomer was diluted to 60 μM in 100 mM HEPES-Tris buffer (pH 7.4) containing 250 mM NaCl (physiological salt condition) and continuously agitated (800 rpm) until the presence of $A\beta_{1-40}$ fibrils was confirmed. To verify, aliquots of the aggregation mixture were removed and diluted in a 7-fold excess of thioflavin T (ThT). ThT is a fluorescent dye that has an enhanced shift in fluorescence in the presence of amyloid's β-sheet structure. Measurements of the fibril mixture were taken using a LS-45 luminescence spectrometer (Perkins Elmer, Inc., Waltham, MA) with an excitation of 450 nm. Fluorescence was calculated by the integration of fluorescence emission spectra from 470 nm to 500 nm and was used to calculate the concentration of fibrils present by

comparing the area under the curve for the aggregation mixture to the area under the curve for the fraction of insoluble fibrils. To produce smaller aggregates, an aliquot of fibrils was sonicated for 5 min. Sonicated $A\beta_{1-40}$ fibrils and $A\beta_{1-40}$ fibrils were used fresh in assays.

2.5 ATPase Assay

An ATPase assay was used to quantify binding of Aβ to P-gp. When a ligand binds to P-gp, ATP is hydrolyzed and inorganic phosphate (P_i) is released. P-gp is exclusively an efflux transporter; therefore, in this assay flipping the protein-membrane conjugate allows for substrate transport into a vesicle and presentation of P-gp to the bulk solution.

Aβ samples and controls, containing either vehicle (negative control) or 20 μM verapamil (positive control), were prepared in 100 mM HEPES-Tris assay buffer (pH 7.4) containing 50 mM KCl, 2 mM DTT, 2 mM EGTA, and 5 mM sodium azide. All samples were prepared with or without 100 μM NaOV, which blocks the ATP binding site to prevent transport of potential substrates, then combined with inverted vesicles containing 20 μg P-gp (Corning) on a 96-well plate and incubated (37°C, 7 min). 4 mM MgATP was added to each well to initiate active transport via P-gp. After an additional incubation (37°C, 20 min), 30 μL 10% SDS stopped the reaction. To quantify P_i present, 200 μL coloring reagent, 35 mM ammonium molybdate, 15 mM zinc acetate, 10% ascorbic acid was added to each well and incubated (37°C, 20 min). The absorbance of each solution was quantified on a Synergy 2 multi-detection microplate reader (BioTek, Winooski, VT) at 800 nm, and the concentration of P_i was calculated using a phosphate standard curve. The vanadate-sensitive ATPase activity was determined by subtracting the concentration of P_i in an NaOV sample from the concentration of P_i in the respective

non-NaOV sample. Samples were plated in triplicate, and the average was determined. For each condition, the fold-increase was calculated relative to the negative control.

2.6 Media and Cell Lines

MDCK cells (National Institutes of Health, Bethesda, MD) were maintained in Dulbecco's modified Eagle's medium (DMEM) supplemented with 10% fetal bovine serum (FBS), 5 mM L glutamine, 50 units/mL penicillin, 50 μg/mL streptomycin, 4.5 g/L glucose, and 100 mg/L sodium pyruvate. MDCK-MDR1 cells (National Institutes of Health, Bethesda, MD) were also maintained in the above media with the addition of 80 ng/mL colchicine in order to suppress the growth of cells not functionally expressing the additional MDR1 gene into P gp present on the cell membrane[85]. All cultures were maintained at 37°C in a humid atmosphere with 5% CO2 for six weeks, and were passaged every 72 h.

2.7 Hoechst 33342 Accumulation Assay

P-gp is known to have two well-described bindings pockets. The first, called the H-binding site, is characterized for its binding of Hoechst 33342. The rate of accumulation of Hoechst 33342 in MDCK-MDR1 cells describes the binding pocket utilized by $A\beta_{1-42}$ oligomers binding to P-gp. MDCK-MDR1 cells were seeded at a density of 5×10^3 cells/well onto black sided 96-well tissue culture plates (Corning) and were maintained for 48 h in DMEM, supplemented as described in Section 2.6. Cells were subsequently treated with varying concentration of $A\beta_{1-42}$ oligomers in 1% FBS media for 15 min prior to incubation with 10 μM Hoechst 33342 in 1% FBS media. Cells treated with buffer equivalent (phosphate buffer, <0.5% DMSO) served as a vehicle. As a positive

control, cells were treated with verapamil and paclitaxel. Fluorescence readings were obtained using a Synergy 2 multi-detection microplate reader. Fluorescence at 360 ± 40 nm excitation and 485 ± 20 nm emission was measured under temperature-controlled conditions (37°C) after a 90 min for equilibrium to be reached. Results are reported as Hoechst 33342 accumulation relative to the control (Hoechst 33342 alone) ± SE.

2.8 Rhodamine 123 Accumulation Assay

The second P-gp binding site investigated was the R-binding site, characterized for its binding to Rhodamine 123. MDCK-MDR1 cells were seeded at a density of 5×10^3 cells/well onto black-sided 96-well tissue culture plates and were maintained in DMEM, supplemented as described in Section 2.6. Cells were subsequently exposed to varying concentrations of $A\beta_{1-42}$ oligomers diluted in 1% FBS media and incubated (37°C, 30 min). Rhodamine 123 diluted in 1% FBS media was added to each well to achieve a final concentration of 10 μM. Cells treated with buffer equivalent served as a vehicle. As a positive control, cells were treated with cyclosporin A or paclitaxel. After an additional incubation (37°C, 30 min), cells were washed three times with cold 12 mM phosphate buffer (pH 7.4). 200 μL warm 12 mM phosphate buffer (pH 7.4) was added before quantifying fluorescence readings with a Synergy 2 multi-detection microplate reader. Fluorescence at 485 ± 20 nm excitation and 528 ± 20 nm emission was measured. Results are reported as Rhodamine 123 accumulation relative to the control (Rhodamine 123 alone) ± SE.

2.9 Cellular Transport Assay

To confirm the effect of Aβ oligomers on P-gp transport across a cell monolayer, a cellular transport assay was implemented. MDCK-MDR1 cells were seeded at a density of 1 x 10^4 cells/well onto the apical surface of a 24-well plate Thincert membrane (Grenier Bio-one) with a 0.4 μm pore size, 1 x 10^8 cm^{-2} pore density, and 0.336 cm^2 membrane surface area. Cells were maintained for 4 days in DMEM, supplemented as described in Section 2.6. Prior to the start and at the conclusion of the assay, TEER measurements were performed across each membrane to ascertain monolayer integrity. To begin the assay, each donor chamber was loaded with 10 μM Rhodamine 123 and in the presence or absence of 2.5 μM $A\beta_{1\text{-}42}$ oligomers in 1% FBS media, while the receptor chamber received 1% FBS media alone. 25 μL samples were removed from the receptor chamber at 1.5, 3, 4.5, and 6 h and replaced with an equal volume of 1% FBS media. The Rhodamine 123 fluorescence of each sample was quantified using a Synergy 2 multi-detection microplate reader at 485 ± 20 nm excitation and 528 ± 20 nm emission. Concentrations of Rhodamine 123 were calculated using a standard curve and corrected for dilution. The measured concentration of Rhodamine 123 was plotted versus time and a linear regression was applied, where the slope is the rate of Rhodamine 123 appearance in the receptor chamber (dC/dt). The apparent permeability, P_e, of Rhodamine 123 in the presence or absence of $A\beta_{1\text{-}42}$ oligomers is calculated by Equation 2.1:

$$P_e = \frac{dC}{dt}\left(\frac{V}{C_0 A}\right) \qquad \text{Equation 2.1}$$

Here dC/dt is the rate of appearance of Rhodamine 123 in the receptor chamber (μmol/s), V is the volume of the receptor chamber (cm^3), C_0 is the initial

Rhodamine 123 concentration in the donor chamber (μM), and A is the surface area of the membrane (cm^2). P_e is calculated in both the basolateral to apical and apical to basolateral directions. Because P-gp is located on the apical surface of cells, the net efflux can then be determined as the ratio of these P_e values:

$$\text{Net Efflux} = \frac{P_{e,B\rightarrow A}}{P_{e,A\rightarrow B}} \qquad \text{Equation 2.2}$$

A net efflux greater than 1 shows active transport via P-gp.

2.10 Immunocytochemistry

To investigate the effect of Aβ species on P-gp cell surface expression, immunocytochemistry was performed. MDCK-MDR1 cells were seeded onto glass coverslips at a density of 3 x 10^5 cells/well and maintained in DMEM supplemented as described in Section 2.6. After 48 h, cells were treated with 0-0.01 μM Aβ aggregate species. Following 6 h treatment, cells were fixed with 4% paraformaldehyde solution, probed with anti-P-gp (F4), conjugated to Cy3, and stained with DAPI. Anti-P-gp (F4) was specifically chosen due to its recognition of an extracellular loop ensuring that only cell membrane bound P-gp was visualized without cell permeabilization.

Cells were imaged 24 h after mounting to slides with a Nikon Eclipse 80i fluorescent microscope using a 40x objective. For each coverslip, 16 different fields of view were captured for analysis of both the DAPI and TRITC channels. CellProfiler was used to quantify the total number of cells using the DAPI images and determine the fluorescence intensity of each cell using the TRITC images. Parameters used by the pipeline were calibrated to statistically produce the same values as manual cell counts.

2.11 Statistical Analysis

Prism 8 software (GraphPad Software, La Jolla, CA) was used for all statistical analysis. For data sets with two groups an unpaired t-test was used for comparison between samples. For data sets with multiple groups, a one-way analysis of variance (ANOVA) was used with a post hoc Dunnett's analysis to compare all samples to the respective control. $p<0.05$ was considered significant. All values are expressed as the mean ± SE.

CHAPTER 3

BINDING AND TRANSPORT OF Aβ BY P-GLYCOPROTEIN

3.1 Introduction

Defining the clearance mechanism for Aβ from the brain has been of interest in recent years. The ability to target this mechanism could allow for increased removal of Aβ early in the disease state. This reduction in Aβ in the brain would lead to less aggregated Aβ because aggregation is a nucleation dependent process. Aβ is an amphipathic molecule with hydrophobic amino acid residues concentrated in the C-terminal portion of the peptide. Aβ is known to be a substrate of low-density lipoprotein receptor-related protein 1 (LRP-1)[26,103–108]. LRP-1 is expressed on the basolateral side of the BBB therefore this allows Aβ to be transported from the brain into the endothelial cells. However, the mechanism for transport out of the endothelial cells into the blood has not been fully described. Some studies have indicated Aβ might be transported into the blood stream via P-gp[95–101]. However, there is controversy on the conditions required for Aβ transport via P-gp. Some of this controversy may be due to lack of Aβ aggregate species characterization.

P-gp, also known as multidrug resistance protein 1 (MDR1), is a membrane bound efflux protein on the apical side of the BBB with a wide variety of amphipathic, hydrophobic substrates, and therefore Aβ is an ideal candidate for transport[44–47]. A member of the ATP-binding cassette transporter superfamily, P-gp is known to have to have 2

"cassettes," each with its own substrate binding site and ATP binding site connected via a short peptide linker[50,55–59,109]. Currently, most studies have determined that P-gp substrates enter the binding sites not from the cytoplasm but instead from the interior of the lipid bilayer.

This chapter identifies and characterizes the P-gp binding capabilities of different Aβ species, including monomer, oligomer, sonicated fibril, and fibril. Using an ATPase activity assay, P-gp was illustrated to selectively bind Aβ oligomers. In order to further elucidate the binding relationship between Aβ oligomers and P-gp, the preferred binding site for Aβ oligomers was investigated. P-gp has two well-described binding sites, each named for a fluorescent substrate. The H-binding site is characterized for its binding relationship with Hoechst 33342[57,61,68,72,73], while the R-binding site is characterized for its binding to Rhodamine 123[34,46,61,66,68,74–77]. An increase in cellular accumulation of Rhodamine 123 in the presence of Aβ oligomers signifies Aβ oligomers interact with P-gp's R-binding site. However, in a cellular transport assay, this relationship was unable to be confirmed. Together, this data displays P-gp's selective binding to Aβ oligomeric species with interaction occurring at the R-binding site but is unable to confirm an effect on the directionality of Rhodamine 123 transport. These results exhibit the continued need for further study of P-gp as a potential therapeutic target for AD.

3.2 Materials and Methods

3.2.1 Preparation of Aβ Aggregate Species

Aggregate species – monomer, oligomer, sonicated fibril, and fibril - were freshly prepared as described, respectively, in Sections 2.2, 2.3, and 2.4.

3.2.2 ATPase Activity Assay

To determine if Aβ aggregate species are interacting with the binding site of P-gp, an ATPase activity assay was used as described in Section 2.5. Aβ monomer, sonicated fibril, and fibril samples were evaluated at 1, 5, and 10 μM. Aβ oligomer samples were evaluated at 0.5, 1, and 5 μM, reflecting the highest concentration of oligomer preparation that remains stable. Results are reported as a fold increase of the ATPase activity relative to buffer alone (VEH), and as the average ± SE.

3.2.3 Cell Culture

To explore the interactions between Aβ oligomers and P-gp in a cell model, both MDCK and MDCK-MDR1 cell lines were used. The MDCK-MDR1 cell line is a variation of the MDCK line that has been transfected to express additional human P-gp. As shown in Figure 3.1, MDCK-MDR1 cells present significantly more P-gp (red staining) on the cell membrane for transport than MDCK cells. Cells were seeded and maintained as described in Section 2.6.

3.2.4 Hoechst 33342 Accumulation Assay

The interaction of Aβ oligomers with the H-binding site of P-gp was investigated using a Hoechst 33342 accumulation assay as described in Section 2.7. MDCK-MDR1 cells were seeded and maintained as described in Sections 2.6 and 2.7. Paclitaxel and verapamil (Figure 3.2) were each examined as positive controls; cells were treated with 1-40 μM paclitaxel or verapamil. 0.5-5 μM Aβ oligomers were evaluated to determine their ability to interact with the H-binding site and increase Hoechst 33342 accumulation.

Results are reported as a fold increase of Hoechst 33342 fluorescence accumulation relative to cells treated with Hoechst 33342 alone (control) and as the average ± SE.

3.2.5 Rhodamine 123 Accumulation Assay

Potential interaction with the R-binding site of P-gp was determined using a Rhodamine 123 accumulation assay as described in Section 2.8. MDCK-MDR1 cells were seeded and maintained as described in Sections 2.6 and 2.8. Paclitaxel and cyclosporin A (Figure 3.2) were each examined as positive controls; cells were treated with 1-40 μM paclitaxel or cyclosporin A. 0.5-5 μM Aβ oligomers were evaluated to determine their ability to interact with the R-binding site and increase Rhodamine 123 accumulation. Results are reported as a fold increase of Rhodamine 123 fluorescence accumulation relative to a sample of Rhodamine alone (control) and as the average ± SE.

3.2.6 Rhodamine 123 Transport Assay

In order to confirm the directionality of Rhodamine 123 transport inhibition, a Rhodamine 123 transport assay was performed as described in Section 2.9. MDCK-MDR1 cells were seeded and maintained as described in Sections 2.6 and 2.9. Rhodamine 123 was added to either the basolateral or apical compartment to measure transport across the cellular monolayer, and treatment in the presence or absence of 2.5 μM Aβ oligomers facilitated examination of R-binding site interactions. After treatment samples were taken from the receiving chamber every 90 min over 6 h to quantify the transport rate of Rhodamine 123 and calculate the apparent permeability, P_e, of Rhodamine 123 from Equation 2.1 in both the basolateral to apical direction and the apical to basolateral

direction, as well as the associated net efflux using Equation 2.2. Net efflux greater than 1 indicates active transport via P-gp. All values are reported as the average ± SE.

3.3 Results

3.3.1 Aβ oligomers bind P-glycoprotein

To evaluate the ability of different Aβ aggregate species to bind to P-gp, an ATPase activity assay was used. Since P-gp is a transmembrane efflux transporter, inverted vesicles with P-gp presenting to the bulk solution were used to determine binding to P-gp. When P-gp vesicles were allowed to interact with Aβ monomer, sonicated fibril, and fibril, insignificant ATPase activity was observed, indicating an absence of P-gp binding (Figure 3.3). Aβ oligomer at 5 μM, however, shows a significant increase in ATPase activity compared to the vehicle (Figure 3.3). These results demonstrate that P-gp selectively binds oligomeric Aβ.

3.3.2 Aβ oligomers exclusively interact with P-glycoprotein's R-binding site

To determine whether Aβ oligomers interact with P-gp's H-binding site or R-binding site, Hoechst 33342 and Rhodamine 123 accumulation assays were used. In this assay, when a potential substrate interacts with the H-binding site, more Hoechst 33342 will accumulate in the cell when compared to a solution with Hoechst 33342 alone (control) due to the potential substrate competing with Hoechst 33342 for the available P-gp H-binding sites. Similarly, when a potential substrate interacts with the R-binding site, more Rhodamine 123 will accumulate in the cell compared to Rhodamine 123 alone (control). Verapamil is known to bind to the H-binding site of P-gp and is shown here to

significantly increase the accumulation of Hoechst 33342 in a dose dependent manner (Figure 3.4C). Cyclosporin A is a known substrate of the R-binding site and shows a significant increase of Rhodamine 123 accumulation (Figure 3.4D). Paclitaxel occupies both the H- and R-binding sites of P-gp and induces a significant increase in both Hoechst 33342 and Rhodamine 123 accumulation (Figure 3.4E). Some cooperativity can also be observed between the two sites. While Rhodamine 123 does not bind to the H-binding site, it does significantly decrease the accumulation of Hoechst 33342 (Figure 3.4A). In contrast however, the presence of Hoechst 33342, does not induce a change in Rhodamine 123 accumulation (Figure 3.4B).

When Aβ oligomers were introduced into these assays, the accumulation of Hoechst 33342 was unaffected (Figure 3.4F). Therefore, Aβ oligomers do not appear to interact with the H-binding site of P gp (Figure 3F). In contrast, the accumulation of Rhodamine 123 increases significantly in the presence of 5 μM Aβ oligomers (Figure 3.4F). These results demonstrate that Aβ oligomers exclusively interact with the R-binding site of P-gp and do not present cooperativity with the H-binding site.

3.3.4 Aβ oligomers have minimal effect on Rhodamine 123 transport across a cell monolayer

To confirm the directionality of transcellular Rhodamine 123 transport via P-gp and examine the effect of Aβ on this transport, a cellular transport assay was performed in MDCK-MDR1 cells. When Rhodamine 123 was added alone to the basolateral chamber a P_e of 7.40 cm/s was measured. In contrast, addition of Rhodamine 123 to the apical chamber led to a much smaller P_e of 1.76 cm/s, thus yielding a net efflux of 4.26. This net efflux is representative of directional transport in the basolateral to apical direction. When

this transport occurred in the presence of 2.5 μM Aβ oligomers, the permeability and the net efflux of Rhodamine 123 in the basolateral to apical direction is slightly decreased (Figure 3.5); however, this difference did not reach significance. These results demonstrate the directionality of Rhodamine 123 transport but fail to confirm the interaction between Aβ oligomers and the P-gp R-binding site in this cell configuration.

3.4 Discussion

Multiple studies report that Aβ interacts with P-gp[95–101]. However, these studies do not compare the ability of different Aβ aggregate states to preferentially bind to P-gp. Here, an ATPase assay was used to demonstrate that Aβ monomer, sonicated fibril (representing soluble intermediates), and fibril do not bind P-gp, while Aβ oligomers exhibit significant binding. Furthermore, Aβ oligomers were shown in a cellular assay to interact exclusively with the R-binding site of P-gp. However, this interaction did not manifest in an assay measuring directional transport across a cellular monolayer.

The lack of binding for the Aβ sonicated fibril and fibril could be due to the sizing of the P-gp binding sites[46,57,61–65]. Specifically, due to the large size of the sonicated fibril and fibril species, those aggregates may not be able to access the binding sites for transport. The ability of smaller Aβ oligomeric species to bind P-gp may be potentially due to Aβ oligomers' ability to insert into the lipid bilayer. Some studies have shown that potential P-gp substrates enter the binding sites through the lipid bilayer instead of directly from the cytoplasm. Additionally, compared to monomer, oligomers present a hydrophobic surface, which may aid in the oligomeric species' preferential binding to P-gp.

P-gp has two well-described transmembrane binding sites, each named for a fluorescent substrate. The H-binding site has been characterized for its binding with

Hoechst 33342[57,61,68,72,73], while the R-binding site has been characterized for its binding with Rhodamine 123[34,46,61,66,68,74–77]. Potential substrates can bind either the H-binding site, the R-binding site, or both to be transported via P-gp. The controls (verapamil[55,57,61,65,66,90,110–112], cyclosporin A[55,57,111,113], paclitaxel[55,61,111,114]) illustrate this binding ability with significant accumulation of Hoechst 33342, Rhodamine 123, or both, respectively.

Additionally, it is shown that Rhodamine 123 and Hoechst 33342 bind only to their respective sites with the possibility of a cooperative relationship between the two binding sites. There is no difference in accumulation of Rhodamine 123 in the presence of Hoechst 33342. When measuring Hoechst 33342 accumulation in the presence of Rhodamine 123, there is a decrease in Hoechst 33342 accumulation, which has been previously studied[68]. This result shows that there can be a cooperative binding relationship between the two binding sites; however, it is not required to have both binding sites occupied for transport to occur. In the case of Aβ oligomers, there is no interaction with the H-binding site, unlike the trends seen with verapamil[55,57,61,65,66,90,110-112], only with the R-binding site, shown by the increase in Rhodamine 123 accumulation similar to the behavior exhibited by cyclosporin A[55,57,111,113]. Additionally, since there is no decrease in Hoechst 33342 accumulation in the presence of Aβ oligomers, there is not a cooperative binding relationship. This adds Aβ oligomers to the list of P-gp substrates that exclusively interact with the R-binding site including cyclosporin A, Rhodamine 123, and others.

The effect of Aβ on directional transport was explored by examining Rhodamine 123 transport via P-gp across a cell monolayer. While directional transport of Rhodamine 123 was confirmed, the reduction of this transport in the presence of Aβ

oligomers does not reach significance. However, the highest manageable concentration in this experiment is lower than that used in the ATPase activity assay and cellular accumulation assays, which did show significant interaction with P-gp.

This study has shown that Aβ oligomers are able to bind to P-gp, instigating the conformational shift for substrate transport. However, other Aβ aggregate species do not show a similar binding ability. Additionally, this work demonstrates that Aβ oligomers interact with the R-binding site of P-gp by decreasing the transport of Rhodamine 123. Together, these findings illustrate the potential of P-gp to be a novel therapeutic target for AD.

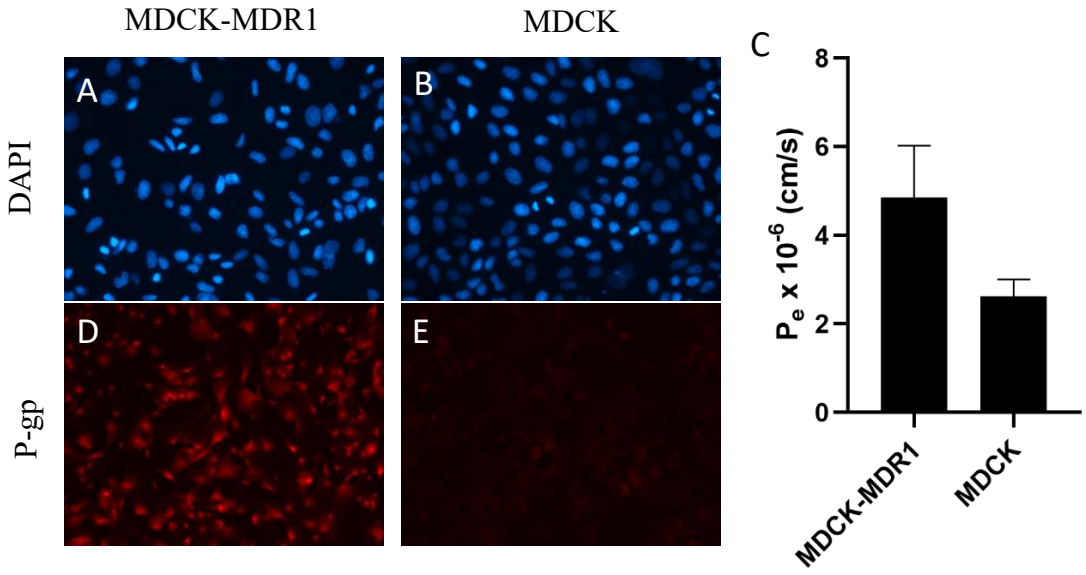

Figure 3.1 P-gp expression and function in MDCK-MDR1 and MDCK cells. MDCK-MDR1 cells are MDCK cells transfected to overexpress P-gp. MDCK-MDR1 cells (panels A, D) exhibit more P-gp staining than MDCK cells (panels B, E). The basolateral to apical permeability coefficient of Rhodamine 123 across a cellular monolayer is greater in MDCK-MDR1 cells than in MDCK cells due to the presence of additional P-gp (panel C).

A

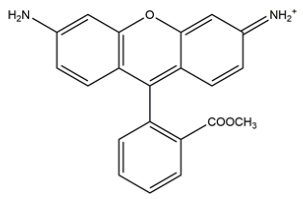

B

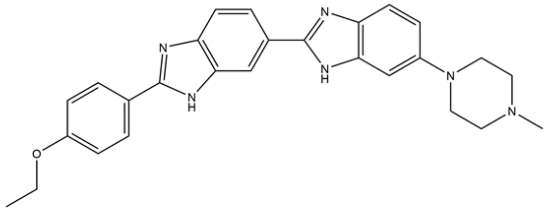

C

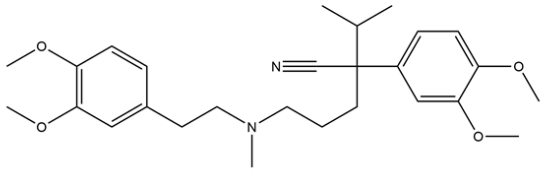

D

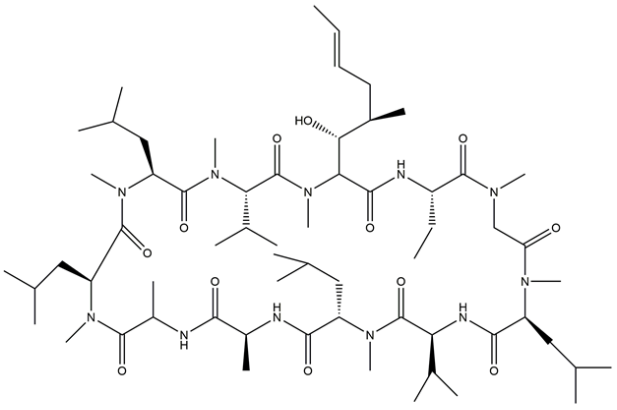

E

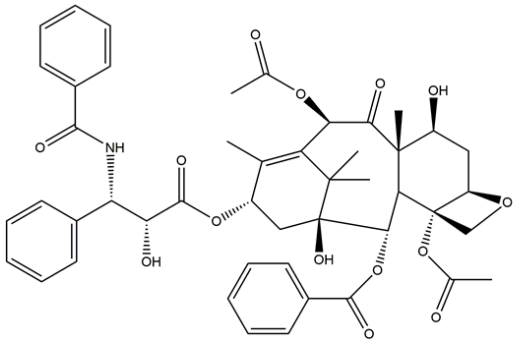

Figure 3.2 Structures of P-gp substrates. Structures of Rhodamine 123 (panel A), Hoechst 33342 (panel B), verapamil (panel C), cyclosporin A (panel D), paclitaxel (panel E), each is a substrate of P-gp.

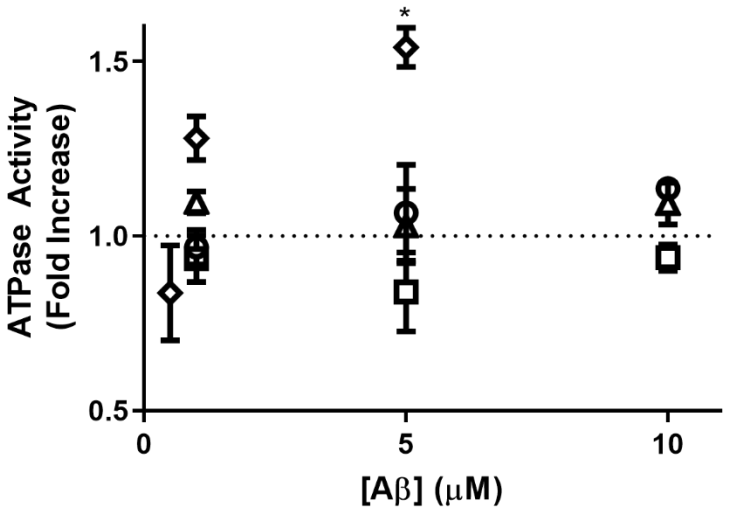

Figure 3.3 ATPase activity of Aβ aggregate species. Aβ monomer (circles), oligomers (diamonds), sonicated fibrils (triangles), and fibrils (squares) were incubated in the presence of inverted P-gp vesicles and MgATP for 20 min. ATPase activity was calculated from Pi generation and reported as a fold increase relative to buffer alone (VEH) indicated by a dashed line and indicative of no binding to P-gp. Error bars indicate SEM, n=3-4. * $p<0.05$.

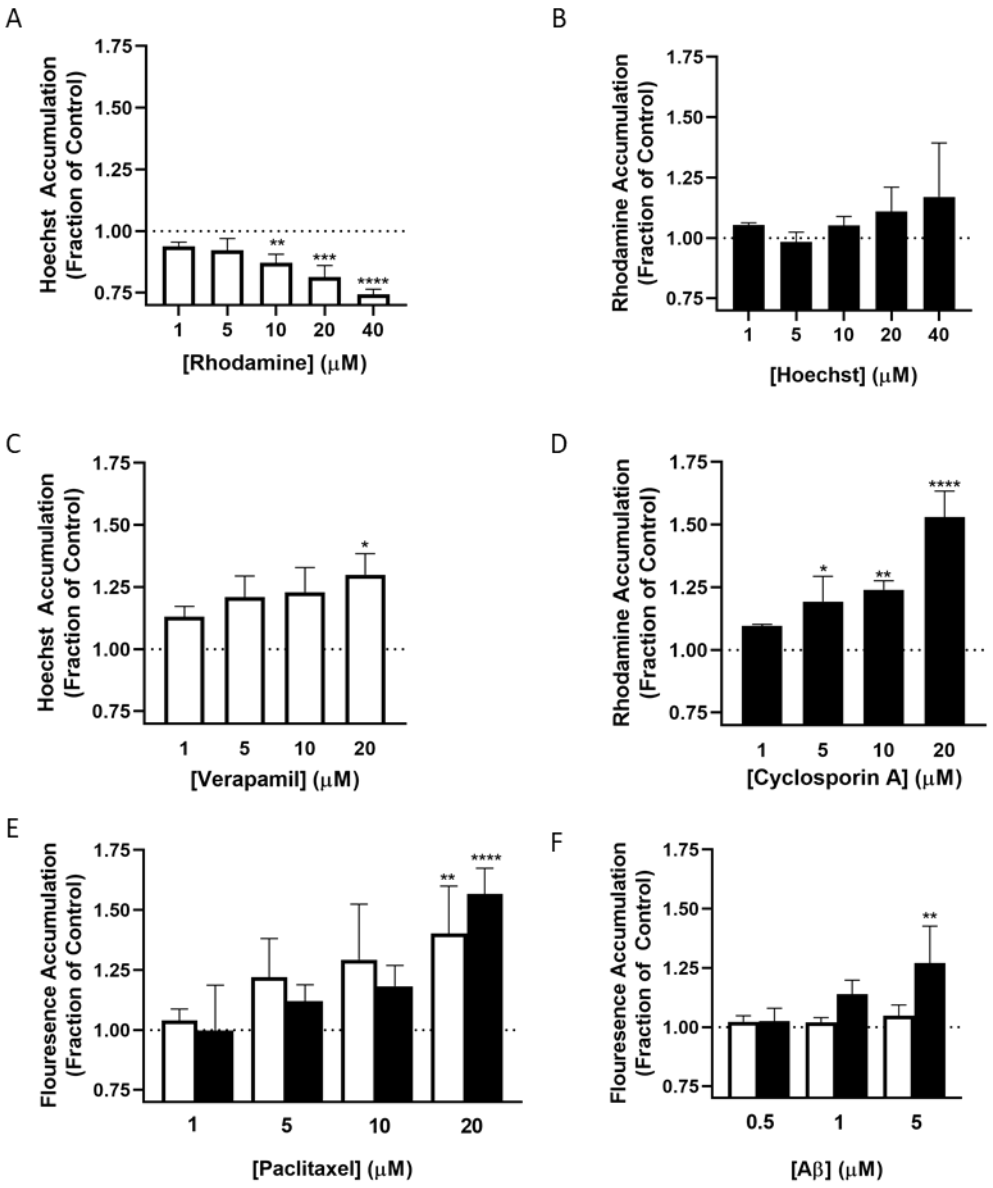

Figure 3.4 Cellular accumulation of Hoechst 33342 or Rhodamine 123 in the presence of alternate P-gp substrates. MDCK-MDR1 cells were pre-incubated in the presence of a competing P-gp substrate, Rhodamine 123 (panel A), Hoechst 33342 (panel B), verapamil (panel C), cyclosporin A (panel D), paclitaxel (panel E), or Aβ oligomers (panel F). 10 μM Hoechst 33342 (open bars) or 10 μM Rhodamine 123 (closed bars) were added to the cells, and incubation continued for 90 or 30 min, respectively to allow for equilibrium to be attained. Fluorescence accumulation is reported as a fraction of the control (Hoechst 33342 or Rhodamine 123 alone), represented by the dashed line at 1 and indicative of basal dye accumulation. Error bars indicate SEM, n=2-4. * $p<0.05$, ** $p<0.01$, *** $p<0.001$, **** $p<0.0001$.

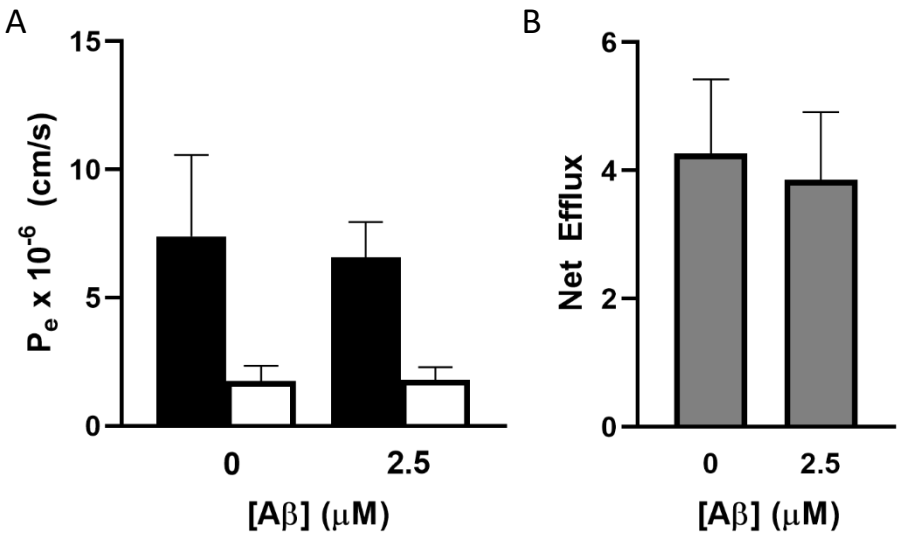

Figure 3.5 Permeability coefficient and net efflux of Rhodamine 123 across MDCK-MDR1 monolayers. Rhodamine 123 transport was measured across MDCK-MDR1 monolayers in the presence and absence of 2.5 μM Aβ oligomers. Cells were grown on a suspended membrane. Following formation of a confluent monolayer, Rhodamine 123 was added to either the basolateral (solid bars) or apical (open bars) chamber. A) Samples were removed from the opposite chamber every 90 min over 6 h to calculate the transport rate of Rhodamine 123 into the receiving chamber. Results are reported as the permeability coefficient, calculated from the transport rate as described in Equation 3.1. B) Net efflux is the ratio of the permeability coefficient in the basolateral to apical direction and the permeability coefficient in the apical to basolateral direction. Results are reported as the average. Error bars indicate SEM, n=4.

CHAPTER 4

REDUCTION OF P-GLYCOPROTEIN TRANSPORT VIA Aβ

4.1 Introduction

One potential clearance mechanism for Aβ from the brain is via P-gp, a membrane bound efflux protein located on the apical side of the BBB[28,115,116]. A minimal presence of P-gp on the BBB has been correlated to a localized high incidence of Aβ plaques[93,94]. While the decreased presence of P-gp could cause the increased concentration of Aβ, other studies demonstrated that Aβ is able to influence P-gp cell surface presence[102,117–120]. Specifically, one study concluded that treatment with Aβ solutions initiated signaling for P-gp degradation via the ubiquitin-proteasome pathway[102].

This chapter investigated whether various Aβ aggregate species are responsible for initiating P-gp degradation and examines the subsequent effect on transport. In order to determine the effect of different Aβ species, cell membrane P-gp is probed using immunocytochemistry. Additionally, cellular accumulation assays are used to ascertain any effect of the Aβ treatments on the ability of P-gp to transport well known substrates. Finally, the effect on directional transport by P-gp across a cell monolayer is probed.

In an MDCK-MDR1 cell culture model, none of the Aβ aggregate species explored demonstrated any effect on the presence of P-gp on the cell membrane. In order to further investigate the transport capabilities of P-gp after treatment with Aβ species, a cellular accumulation assay was performed following Aβ treatment. Again, none of the Aβ species

revealed any difference in cellular accumulation of P-gp substrates. In the cellular transport assay, however, each of the Aβ species tested had a deleterious effect on the net efflux of Rhodamine 123. Uniquely, this assay allows cell treatment at the basolateral surface to more directly mimic the conditions of the diseased brain.

Together, this data describes an interesting relationship between P-gp and Aβ. When Aβ is present at the apical surface of a cellular monolayer, the presence of P gp is unaltered. However, when the Aβ species are present at the basolateral surface of the cell, consistent with pathology in the AD brain, the transport via P-gp is reduced. These results exhibit the complexity of the relationship between Aβ and P-gp and the need for further study of this relationship to fully understand the role of P-gp in the AD brain.

4.2 Materials and Methods

4.2.1 Preparation of Aβ Aggregate Species

Aggregate species – monomer, oligomer, protofibril mix, and fibril – were freshly prepared as described, respectively, in Sections 2.2, 2.3, and 2.4.

4.2.2 Cell Culture

To explore the interactions between Aβ aggregates and P-gp in a cell model, the MDCK-MDR1 cell line was used. Cells were seeded and maintained as described in Section 2.6.

4.2.3 Immunocytochemistry

To determine the impact of extended treatment with Aβ aggregates on the available membrane-bound P-gp, immunocytochemistry was used as described in Section 2.10. MDCK-MDR1 cells were seeded onto coverslips and maintained as described in Section 2.6 and 2.10. Cells were treated for 6 h with 0-0.01 μM Aβ aggregate species on the apical surface. After treatment, cells were fixed and stained with DAPI and an anti-P-gp (F4), a P-gp antibody which binds to an extracellular loop of P-gp. Images were analyzed with CellProfiler to quantify P-gp signal per cell. Average values are reported as P-gp per cell relative to the vehicle ± SE.

4.2.4 Hoechst 33342 and Rhodamine 123 Accumulation Assays

To determine if extended Aβ treatment leads to a reduction in functional P-gp present on the cell membrane, a Hoechst 33342 or Rhodamine 123 accumulation assay was used as described in Section 2.7 and 2.8. MDCK-MDR1 cells were seeded and maintained as described in Sections 2.6, 2.7, and 2.8. Cells were treated on the apical surface with 0-0.01 μM Aβ aggregates for 6 h prior to introduction of Hoechst 33342 or Rhodamine and assessment of accumulation. A decrease in accumulation compared with the vehicle would attest to a reduction in functional P-gp in the presence of Aβ aggregate species. Results are reported as a fold increase of Hoechst 33342 or Rhodamine 123 fluorescence accumulation relative to the vehicle and as the average ± SE.

4.2.5 Rhodamine 123 Transport Assay

In order to explore the effect of extended Aβ treatment on directionality of the transport of Rhodamine 123 via P-gp, a Rhodamine 123 transport assay was used as described in Section 2.9. MDCK-MDR1 cells were seeded and maintained as described in Sections 2.6 and 2.9. MDCK-MDR1 monolayers were treated with in the presence or absence of 0.001 μM Aβ aggregates for 6 h in the basolateral chamber to mimic the amyloid plaques' location in the brain. After the treatment was removed, 10 μM Rhodamine 123 solution was placed in either the apical or basolateral chamber to measure Rhodamine 123 transport across the cellular monolayer. Samples were taken every 90 min over 6 h to quantify the transport rate of Rhodamine 123 and calculate the apparent permeability, P_e, of Rhodamine 123 from Equation 2.1 in the basolateral to apical direction and the apical to basolateral direction, as well as the associated net efflux using Equation 2.2. Net efflux greater than 1 indicates active transport via P-gp. All values are reported as the average ± SE.

4.3 Results

4.3.1 Aβ aggregates do not affect the presence of P-gp on the cell membrane

In order to quantify the change in the presence of P-gp present on the cell membrane, immunocytochemistry was used. The anti-P-gp chosen binds to an extracellular loop of P-gp allowing for exclusive visualization of the protein embedded in the cell membrane instead of the total protein after permeabilizing the membrane. After treating the apical surface of the cells with 0.001-0.01 μM Aβ oligomer, fibril mix, and fibril, cells displayed no difference in P-gp present on the cell membrane (Figure 4.1).

4.3.2 Aβ aggregates do not affect the accumulation of either Hoechst 33342 or Rhodamine 123

The functionality of P-gp present on the cell membrane was examined with a Hoechst 33342 or Rhodamine 123 accumulation assay. In this assay, the accumulation of the fluorescent substrate was compared between cells which had received 0-0.01 μM Aβ monomer, oligomer, protofibril mix, or fibril. Cells probed with Hoechst 33342 exhibit no additional accumulation compared with the vehicle (Figure 4.2A). Likewise, cells examined with Rhodamine 123, showed minimal accumulation difference from the vehicle (Figure 4.2B).

4.3.3 Aβ aggregates effect the net efflux of Rhodamine 123

To evaluate the effect of Aβ aggregate species when treating the basolateral surface of the cells, mimicking the situational environment of AD at the BBB, a Rhodamine 123 transport assay was used. Minimal differences appear in the apical to basolateral permeability coefficient for any of the treatments compared to the vehicle (Figure 4.3A, open bars), while there are slight differences exhibited in the basolateral to apical permeability coefficients compared to the vehicle (Figure 4.3A, closed bars). When considering the net effluxes of each treatment, there is a clear difference between each of the Aβ aggregate species and the vehicle treatment.

4.4 Discussion

Previously, an inversely correlative relationship was described between Aβ plaques and P-gp at the BBB[93,94]. Later, it was demonstrated Aβ had a deleterious effect on the

presence of P gp on the cell membrane[102,117,119–121]. However, this study did not fully investigate the different Aβ aggregate states that were responsible for this effect. Here, the purpose is to compare the effect of Aβ aggregate species on the presence of P-gp on the cell membrane. While Aβ treatment at the apical surface of cells did not yield any effect on P-gp presence at the cell membrane, when MDCK-MDR1 cells are treated at the basolateral surface, a reduction of transport via P-gp is observed.

Immunocytochemistry and cellular accumulation assays indicate that there is no difference in either P-gp cell surface expression or P-gp substrate accumulation after treatment with Aβ aggregate species. Two potential explanations for this result are either Aβ does not influence the presence of P-gp on the cell membrane and its transport abilities, or Aβ is unable to instigate its potential reductive effects from the apical surface of these cells.

In order to test the hypothesis that Aβ's reductive influence on P-gp requires action on the basolateral surface of the cells, MDCK-MDR1 cells were grown on a suspended semi-permeable membrane to allow treatment at the basolateral surface. Here, the net efflux of Rhodamine 123 was reduced following each Aβ species treatment, demonstrating the deleterious effect of Aβ.

BBB endothelial cells are known to exhibit apicobasal polarity where the lipid and protein composition of the cell membrane is highly dependent on location[122]. While these experiments were performed in non-brain microvasculature endothelial cells, MDCK-MDR1 cells do display polarity, especially when grown on a suspended membrane[83,86]. Thus, the trends shown here in MDCK-MDR1 cells exploiting the polarity of the cellular structure may be increased in a BBB endothelial model.

Together, this study illustrates the importance of mimicking the local conditions in the diseased brain due to the intrinsic polarity of the cells. Additionally, it conveys the need for further inquiry into the role P-gp plays in the AD disease state.

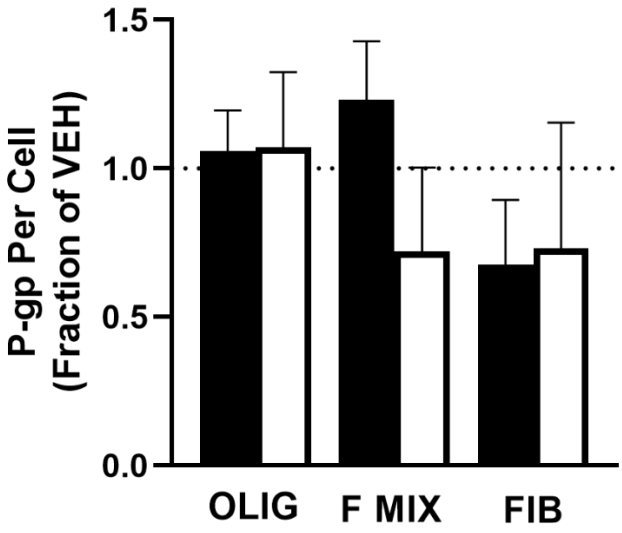

Figure 4.1 P-gp presence on the cell membrane after Aβ treatment. MDCK-MDR1 cells grown on coverslips were treated with 0.001 μM (closed bars) or 0.01 μM (open bars) Aβ oligomer, fibril mix or fibril for 6 h. Cells were then washed, fixed, and probed with DAPI and anti-P-gp (P7965) conjugated to Cy3. Images were analyzed using CellProfiler to determine Cy3 staining per cell relative to the cells treated with buffer alone (VEH) represented by a dashed line at 1. Error bars represent SEM, n=2-3.

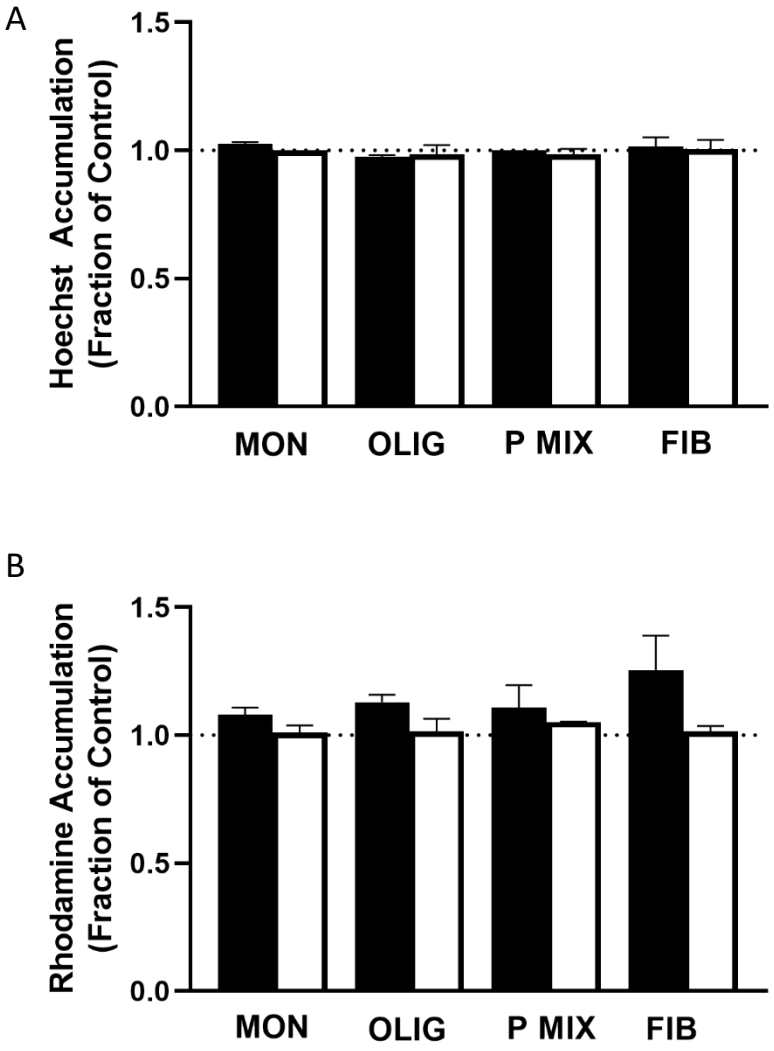

Figure 4.2 Cellular accumulation of Hoechst 33342 or Rhodamine 123 in MDCK-MDR1 cells after treatment with Aβ treatment. MDCK-MDR1 cellular monolayers were treated with 0.001 μM (closed bars) or 0.01 μM (open bars) Aβ monomer, oligomer, protofibril mix or fibril for 6 h, then washed. 10 μM Hoechst 33342 (panel A) or 10 μM Rhodamine 123 (panel B) was added to the cells for 30 or 90 min, respectively to allow for equilibrium to be attained. Fluorescence accumulation is reported as a fraction of the vehicle, represented by a dashed line at 1. Error bars represent SEM. n=2.

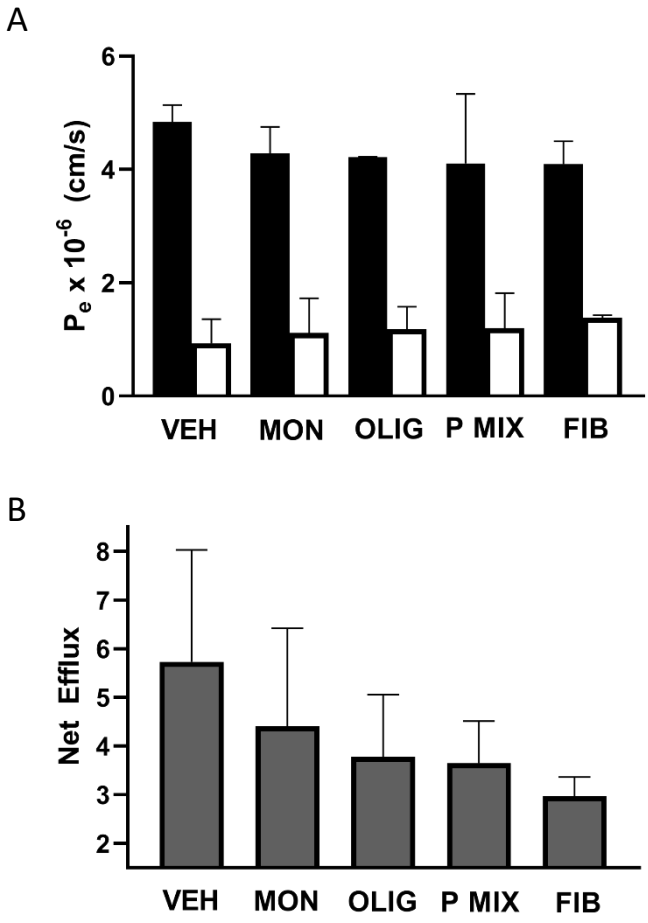

Figure 4.3 Permeability and net efflux across MDCK-MDR1 cellular monolayers after Aβ treatment. MDCK-MDR1 monolayers grown on a suspended membrane were treated with buffer (VEH) or 0.001 μM Aβ monomer (MON)), oligomer (OLIG), protofibril mix (P MIX), or fibril (FIB), for 6 h via addition of Aβ to the basolateral chamber. After treatment, Rhodamine 123 was added to either the basolateral or apical chamber. A) Samples were removed from the opposite chamber every 90 min over 6 h to calculate the permeability coefficient in the basolateral to apical direction (solid bars) and the apical to basolateral direction (open bars). B) These permeability coefficients were used to calculate the net efflux. n=2.

CHAPTER 5

CONCLUSIONS

With an aging population, in addition to the increase in average life-span, the number of AD cases will only continue to increase. As of 2018, 5.8 million Americans are living with Alzheimer's disease, this number is expected the increase to almost 14 million by the year 2050[1]. Since the only current medications available for AD patients treat the symptoms and not the underlying disease pathology, the need for a therapeutic is urgently increasing as well. In conjunction, a more complete understanding of the underlying disease state is required in order to properly target those therapeutics. Fully describing the clearance mechanism of AD's Aβ species is one pathway to a more fundamental understanding of the disease state. Therefore, this study aimed to elucidate the relationship between P-gp and Aβ.

In Chapter 3, it was demonstrated that P-gp selectively binds to Aβ oligomeric species. Additionally, Aβ oligomers were verified as selectively interacting with P-gp's R-binding site, indicated by increased accumulation of Rhodamine 123 but not Hoechst 33342 in a cellular monolayer. However, when investigating the directional Rhodamine 123 transport across a cellular monolayer, competition with Aβ oligomers for the R-binding site could not be confirmed.

In Chapter 4, the effect of all Aβ species on the presence of P-gp on the cell membrane was analyzed. When measuring P-gp's cell membrane presence both directly, via immunocytochemistry, and indirectly, via cellular accumulation and transport, an

interesting trend emerged within immunocytochemistry and cellular accumulation assays, the apical surface of the cellular monolayer was treated with the Aβ species. In all cases, there was no significant alteration in P-gp presence compared with the vehicle, regardless of the aggregate species. However, in the cellular transport assay, the cellular monolayers are grown on a suspended semi-permeable membrane, making the basolateral surface of the cells available for treatment. In these cellular transport assays, a difference in transport capabilities was observed between the vehicle and each Aβ species. This variance in results correlating with the cell surface treated is especially interesting when considering the disease state. P-gp is located on the apical surface of the brain microvasculature, while the Aβ plaques as well as smaller aggregates are located at the basolateral surface of those capillaries. The cellular transport assay best represents what is potentially occurring in the brain during the disease state.

In summary, this study has characterized Aβ's interaction with P-gp in two distinct pathways. First, results demonstrated P-gp selectively interacting with Aβ oligomers at the R-binding site as a potential clearance mechanism. Second, experimentation probed a possible deleterious relationship between Aβ species and P-gp's presence on the cell membrane. These findings will direct future work investigating P-gp as a potential therapeutic target for AD.

CHAPTER 6

FUTURE PERSPECTIVES

While Aβ oligomeric species have been illustrated to interact with P-gp's R-binding site in this study, this interaction was defined by a reduction in Rhodamine 123 transport. In order to conclusively show that Aβ oligomers are transported via P-gp, a more direct measurement of Aβ oligomers needs to occur. One potential solution is the labelling of Aβ in order to directly measure its binding and transport. However, the aggregation abilities of pre-labelled monomeric Aβ are not well studied and it is believed that the oligomerization sites might be altered by the conjugated fluorescent dye. Additionally, the labelling of oligomeric Aβ was investigated during the course of this study. This was ultimately unsuccessful due to the low protein yield and high excess dye concentration present in the samples. Alternatively, current protocols utilize sandwich ELISAs, which are not without their own difficulties. These assays leverage antibodies that can have issues recognizing Aβ oligomers due to potentially masked binding sites. This complication might be solved with dissociation of oligomeric aggregates in basic buffer. Future work will explore these possibilities to confirm Aβ oligomeric transport before P-gp can serve as a potential therapeutic target for AD.

Additionally, these findings should be verified in a BBB cell system and animal-based models. As stated previously, the MDCK/MDCK-MDR1 cell models are able to model the function of P-gp as seen on the BBB, but as canine kidney cells they do not exhibit all of the functions of the human BBB. The first step would be to verify the

transport findings in a primary human brain microvascular endothelial cell (HBMVEC) model. Then, continue into a mouse model overexpressing a human MDR1 gene such as hMDR1-MAC due to the differences between mouse and human P-gp specifically in transport across the BBB[109].

With positive future work results, P-gp should be investigated as a potential therapeutic target for AD. The loss of P-gp transport across the cell membrane, demonstrated in Chapter 4, will need to be attenuated in order to preserve BBB clearance mechanisms, not only for Aβ but for other potentially harmful substrates as well. Some work has identified potential P-gp cellular presence stimulators[123,124]. Continuing this work will be a novel therapeutic target for AD research. Many previous therapeutic targets have focused on Aβ production or the Aβ aggregation pathway, and these targets required bioactive agents to pass the BBB. With a goal of recovering P-gp levels, the target instead would be the cells of the BBB itself, offering an easier delivery mechanism.

REFERENCES

1. Alzheimer's Association. *2019 Alzheimer's disease facts and figures includes a special report on Alzheimer's detection in the primary care setting: connecting patients and physicians*. (2019).
2. Alzheimer, A. Die diagnostischen Schwierigkeiten in der Psychiatric. *Zeitschrift fer die gesamte Neurol. und Psychiatr.* **1**, 1–19 (1910).
3. Hippius, H. & Neundorfer, G. The discovery of Alzheimer's disease. *Dialogues Clin. Neurosci.* **5**, 101–108 (2003).
4. Bailey, J. A., Maloney, B., Ge, Y. & Lahiri, D. K. Functional activity of the novel Alzheimer's amyloid β -peptide interacting domain (AβID) in the APP and BACE1 promoter sequences and implications in activating apoptotic genes and in amyloidogenesis. *Gene* **488**, 13–22 (2011).
5. Tanzi, R. E. & Bertram, L. Twenty years of the Alzheimer's disease amyloid hypothesis: A genetic perspective. *Cell* **120**, 545–555 (2005).
6. Ladiwala, A. R. a *et al.* Conformational differences between two amyloid β oligomers of similar size and dissimilar toxicity. *J. Biol. Chem.* **287**, 24765–73 (2012).
7. Jang, J.-H. & Surh, Y.-J. Beta-amyloid-induced apoptosis is associated with cyclooxygenase-2 up-regulation via the mitogen-activated protein kinase-NF-kappaB signaling pathway. *Free Radic. Biol. Med.* **38**, 1604–13 (2005).
8. Ryan, D. a., Narrow, W. C., Federoff, H. J. & Bowers, W. J. An improved method

for generating consistent soluble amyloid-beta oligomer preparations for in vitro neurotoxicity studies. *J. Neurosci. Methods* **190**, 171–179 (2010).

9. Rensink, A. a M. *et al.* Inhibition of amyloid-beta-induced cell death in human brain pericytes in vitro. *Brain Res.* **952**, 111–121 (2002).
10. Walsh, D. M. *et al.* Naturally secreted oligomers of amyloid beta protein potently inhibit hippocampal long-term potentiation in vivo. *Nature* **416**, 535–539 (2002).
11. Walsh, D. M. & Selkoe, D. J. Aβ oligomers - A decade of discovery. *J. Neurochem.* **101**, 1172–1184 (2007).
12. Dahlgren, K. N. *et al.* Oligomeric and fibrillar species of amyloid-β peptides differentially affect neuronal viability. *J. Biol. Chem.* **277**, 32046–32053 (2002).
13. Chromy, B. a *et al.* Self-assembly of Abeta(1-42) into globular neurotoxins. *Biochemistry* **42**, 12749–12760 (2003).
14. Haass, C. & Selkoe, D. J. Soluble protein oligomers in neurodegeneration: lessons from the Alzheimer's amyloid beta-peptide. *Nat. Rev. Mol. Cell Biol.* **8**, 101–112 (2007).
15. Tomic, J. L., Pensalfini, A., Head, E. & Glabe, C. G. Soluble fibrillar oligomer levels are elevated in Alzheimer's disease brain and correlate with cognitive dysfunction. *Neurobiol. Dis.* **35**, 352–8 (2009).
16. Davis, T. J. *et al.* Comparative study of inhibition at multiple stages of amyloid-beta self-assembly provides mechanistic insight. *Mol. Pharmacol.* **76**, 405–13 (2009).
17. Bitan, G. *et al.* Amyloid β-protein (Aβ) assembly : Aβ40 and Aβ42 oligomerize through distinct pathways. *Proc. Natl. Acad. Sci.* **100**, 330–335 (2003).

18. Moore, K. A. *et al.* Influence of gold nanoparticle surface chemistry and diameter upon Alzheimer's disease amyloid-β protein aggregation. *J. Biol. Eng.* **11**, 1–11 (2017).

19. Soto-Ortega, D. D. *et al.* Inhibition of amyloid-β aggregation by coumarin analogs can be manipulated by functionalization of the aromatic center. *Bioorg. Med. Chem.* **19**, 2596–602 (2011).

20. Pate, K. M. *et al.* Anthoxanthin Polyphenols Attenuate Aβ Oligomer-induced Neuronal Responses Associated with Alzheimer's Disease. *CNS Neurosci. Ther.* **23**, 135–144 (2017).

21. Nichols, M. R. *et al.* Growth of Beta-amyloid(1-40) protofibrils by monomer elongation and lateral association. Characterization of distinct products by light scattering and atomic force microscopy. *Biochemistry* **41**, 6115–6127 (2002).

22. Stine, W. B., Dahlgren, K. N., Krafft, G. a. & LaDu, M. J. In vitro characterization of conditions for amyloid-β peptide oligomerization and fibrillogenesis. *J. Biol. Chem.* **278**, 11612–11622 (2003).

23. Lührs, T. *et al.* 3D structure of Alzheimer's amyloid-beta(1-42) fibrils. *Proc. Natl. Acad. Sci. U. S. A.* **102**, 17342–17347 (2005).

24. Tanzi, R. E., Moir, R. D. & Wagner, S. L. Clearance of Alzheimer's Aβ peptide: The many roads to perdition. *Neuron* **43**, 605–608 (2004).

25. Wang, Y.-J., Zhou, H.-D. & Zhou, X.-F. Clearance of amyloid-beta in Alzheimer's disease: progress, problems and perspectives. *Drug Discov. Today* **11**, 931–938 (2006).

26. Zlokovic, B. V, Yamada, S., Holtzman, D., Ghiso, J. & Frangione, B. Clearance of

amyloid beta-peptide from brain: transport or metabolism? *Nat. Med.* **6**, 718–719 (2000).

27. Selkoe, D. J. Translating cell biology into therapeutic advances in Alzheimer's disease. *Nature* **399**, A23–A31 (1999).

28. Begley, D. J. ABC Transporters and The Blood-Brain Barrier. *Curr. Pharm. Des.* **10**, 1295–1312 (2004).

29. Cardoso, F. L., Brites, D. & Brito, M. A. Looking at the blood-brain barrier: Molecular anatomy and possible investigation approaches. *Brain Res. Rev.* **64**, 328–363 (2010).

30. Abbott, N. J., Patabendige, A. A. K., Dolman, D. E. M., Yusof, S. R. & Begley, D. J. Structure and function of the blood-brain barrier. *Neurobiol. Dis.* **37**, 13–25 (2010).

31. Saha, P., Yang, J. J. & Lee, V. H. L. Existence of a p-glycoprotein drug efflux pump in cultured rabbit conjunctival epithelial cells. *Investig. Ophthalmol. Vis. Sci.* **39**, 1221–1226 (1998).

32. Barthe, L., Bessouet, M., Woodley, J. F. & Houin, G. The improved everted gut sac: A simple method to study intestinal P-glycoprotein. *Int. J. Pharm.* **173**, 255–258 (1998).

33. Calcabrini, A. *et al.* Detection of P-glycoprotein in the nuclear envelope of multidrug resistant cells. *Histochem. J.* **32**, 599–606 (2000).

34. Fontaine, M., Elmquist, W. F. & Miller, D. W. Use of Rhodamine 123 to Examine the Functional Activity of P-glycoprotein in Primary Cultured Brain Microvessel Endothelial Cell Monolayers. *Life Sci.* **59**, 1521–1531 (1996).

35. Nakanishi, H., Myoui, A., Ochi, T. & Aozasa, K. P-glycoprotein expression in soft-tissue sarcomas. *J. Cancer Res. Clin. Oncol.* **123**, 352–356 (1997).

36. Juliano, R. L. & Ling, V. A surface glycoprotein modulating drug permeability in Chinese hamster ovary cell mutants. *Biochim. Biophys. Acta* **455**, 152–162 (1976).

37. Horio, M. *et al.* Transepithelial transport of drugs by the multidrug transporter in cultured Madin-Darby canine kidney cell epithelia. *J. Biol. Chem.* **264**, 14880–14884 (1989).

38. Thiebaut, F. *et al.* Cellular localization of the multidrug-resistance gene product P-glycoprotein in normal human tissues. *Proc. Natl. Acad. Sci. U. S. A.* **84**, 7735–7738 (1987).

39. Roninson, I. B. *et al.* Isolation of human mdr DNA sequences amplified in multidrug-resistant KB carcinoma cells. *Proc. Natl. Acad. Sci. U. S. A.* **83**, 4538–42 (1986).

40. Gros, P., Croop, J. & Housman, D. Mammalian multidrug resistance gene: Complete cDNA sequence indicates strong homology to bacterial transport proteins. *Cell* **47**, 371–380 (1986).

41. Gros, P., Neriah, Y. Ben, Croop, J. M. & Housman, D. E. Isolation and expression of a complementary DNA that confers multidrug resistance. *Nature* **323**, 728–731 (1986).

42. Gerlach, J. H. *et al.* Homology between P-glycoprotein and a bacterial haemolysin transport protein suggests a model for multidrug resistance. *Nature* **324**, 485–489 (1986).

43. Ueda, K. *et al.* The mdr1 gene, responsible for multidrug-resistance, codes for P-

glycoprotein. *Biochem. Biophys. Res. Commun.* **141**, 956–962 (1986).

44. Labroille, G. *et al.* Cytometric study of intracellular P-gp expression and reversal of drug resistance. *Cytometry* **32**, 86–94 (1998).

45. Montanari, F. & Ecker, G. F. Prediction of drug-ABC-transporter interaction - Recent advances and future challenges. *Adv. Drug Deliv. Rev.* **86**, 17–26 (2015).

46. Kadioglu, O. *et al.* Interactions of human P-glycoprotein transport substrates and inhibitors at the drug binding domain: Functional and molecular docking analyses. *Biochem. Pharmacol.* **104**, 42–51 (2016).

47. See, Y. P., Carlsen, S. A., Till, J. E. & Ling, V. Increased drug permeability in chinese hamster ovary cells in the presence of cyanide. *Biochim. Biophys. Acta* **373**, 242–252 (1974).

48. Wiese, M. & Stefan, S. M. The A-B-C of small-molecule ABC transport protein modulators: From inhibition to activation—a case study of multidrug resistance-associated protein 1 (ABCC1). *Med. Res. Rev.* 1–51 (2019). doi:10.1002/med.21573

49. Szakács, G. *et al.* Predicting drug sensitivity and resistance: Profiling ABC transporter genes in cancer cells. *Cancer Cell* **6**, 129–137 (2004).

50. Ambudkar, S. V *et al.* Biochemical, cellular, and pharmacological aspects of the multidrug transporter. *Annu. Rev. Pharmacol. Toxicol.* **39**, 361–398 (1999).

51. Wang, E. jia, Casciano, C. N., Clement, R. P. & Johnson, W. W. Two transport binding sites of P-glycoprotein are unequal yet contingent: Initial rate kinetic analysis by ATP hydrolysis demonstrates intersite dependence. *Biochim. Biophys. Acta - Protein Struct. Mol. Enzymol.* **1481**, 63–74 (2000).

52. Johnson, Z. L. & Chen, J. ATP Binding Enables Substrate Release from Multidrug Resistance Protein 1. *Cell* **172**, 81–89 (2018).

53. Horio, M., Gottesman, M. M. & Pastan, I. R. A. ATP-dependent transport of vinblastine in vesicles from human. *Proc. Natl. Acad. Sci.* **85**, 3580–3584 (1988).

54. Urbatsch, I. L., Sankaran, B., Bhagat, S. & Senior, A. E. Both P-glycoprotein nucleotide-binding sites are catalytically active. *J. Biol. Chem.* **270**, 26956–26961 (1995).

55. Sharom, F. J. Shedding light on drug transport: structure and function of the P-glycoprotein multidrug transporter (ABCB1)This paper is one of a selection of papers published in this Special Issue, entitled CSBMCB — Membrane Proteins in Health and Disease. *Biochem. Cell Biol.* **84**, 979–992 (2008).

56. Higgins, C. F., Callaghan, R., Linton, K. J., Rosenberg, M. F. & Ford, R. C. Structure of the multidrug resistance P-glycoprotein. *Semin. Cancer Biol.* **8**, 135–142 (1997).

57. Mollazadeh, S., Sahebkar, A., Hadizadeh, F., Behravan, J. & Arabzadeh, S. Structural and functional aspects of P-glycoprotein and its inhibitors. *Life Sci.* **214**, 118–123 (2018).

58. Cornwell, M. M., Safa, A. R., Felsted, R. L., Gottesman, M. M. & Pastan, I. Membrane vesicles from multidrug-resistant human cancer cells contain a specific 150- to 170-kDa protein detected by photoaffinity labeling. *Proc. Natl. Acad. Sci.* **83**, 3847–3850 (1986).

59. Suvanto, S. P-glycoprotein Characteristics and Investigation of P-glycoprotein Mediated Drug-Drug INteractions with in vitro Methods. (2014).

60. Ambudkar, S. V., Kim, I. W. & Sauna, Z. E. The power of the pump: Mechanisms of action of P-glycoprotein (ABCB1). *Eur. J. Pharm. Sci.* **27**, 392–400 (2006).

61. Martin, C. *et al.* Communication between Multiple Drug Binding Sites on P-glycoprotein. *Mol. Pharmacol.* **58**, 624–632 (2000).

62. Ferreira, R. J., Ferreira, M. J. U. & Dos Santos, D. J. V. A. Insights on P-glycoproteins efflux mechanism obtained by molecular dynamics simulations. *J. Chem. Theory Comput.* **8**, 1853–1864 (2012).

63. Wen, P. C., Verhalen, B., Wilkens, S., Mchaourab, H. S. & Tajkhorshid, E. On the origin of large flexibility of P-glycoprotein in the inward-facing state. *J. Biol. Chem.* **288**, 19211–19220 (2013).

64. Safa, A. R. Identification and characterization of the binding sites of P-glycoprotein for multidrug resistance-related drugs and modulators. *Curr. Med. Chem. Anticancer. Agents* **4**, 1–17 (2004).

65. Pascaud, C., Garrigos, M. & Orlowski, S. Multidrug Resistance Transport P-glycoprotein has Distinct but Interacting Binding Sites for Cytotoxic Drugs and Reversing Agents. *Biochem. J.* **333**, 351–358 (1998).

66. Loo, T. W. & Clarke, D. M. Defining the Drug-binding Site in the Human Multidrug Resistance P-glycoprotein Using a Methanethiosulfonate Analog of Verapamil, MTS-verapamil. *J. Biol. Chem.* **276**, 14972–14979 (2001).

67. Döppenschmitt, S. *et al.* Characterization of binding properties to human P-glycoprotein: development of a [3H]verapamil radioligand-binding assay. *J. Pharmacol. Exp. Ther.* **288**, 348–57 (1999).

68. Tang, F., Ouyang, H., Yang, J. Z. & Borchardt, R. T. Bidirectional Transport of

Rhodamine 123 and Hoechst 33342, Fluorescence Probes of the Binding Sites on P-glycoprotein, across MDCK-MDR1 Cell Monolayers. *J. Pharm. Sci.* **93**, 1185–1194 (2004).

69. Aller, S. G. *et al.* Structure of P-Glycoprotein Reveals a Molecular Basis for Poly-Specific Drug Binding. *Science (80-.).* **323**, 1718–1722 (2009).

70. Litman, T., Zeuthen, T., Skovsgaard, T. & Stein, W. D. Competitive, non-competitive and cooperative interactions between substrates of P-glycoproteins as measured by ATPase activity. *Biochim. Biophys. Acta - Mol. Basis Dis.* **1361**, 169–176 (1997).

71. Dey, S., Ramachandra, M., Pastan, I., Gottesman, M. M. & Ambudkar, S. V. Evidence for two nonidentical drug-interaction sites in the human P-glycoprotein. *Proc. Natl. Acad. Sci. U. S. A.* **94**, 10594–9 (1997).

72. Shapiro, A. B., Corder, A. B. & Ling, V. P-glycoprotein-mediated Hoechst 33342 transport out of the lipid bilayer. *Eur. J. Biochem.* **250**, 115–121 (1997).

73. Shapiro, A. B., Fox, K., Lee, P., Yang, Y. D. & Ling, V. Functional intracellular P-glycoprotein. *Int. J. Cancer* **76**, 857–864 (1998).

74. Robey, R. *et al.* Efflux of rhodamine from CD56+ cells as a surrogate marker for reversal of P-glycoprotein-mediated drug efflux by PSC 833. *Blood* **93**, 306–314 (1999).

75. Johnson, L. V, Walsh, M. L. & Chen, L. A. N. B. Localization of mitochondria in living cells with rhodamine 123. *Proc. Natl. Acad. Sci. U. S. A.* **77**, 990–994 (1980).

76. Loo, T. W. & Clarke, D. M. Location of the rhodamine-binding site in the human

multidrug resistance P-glycoprotein. *J. Biol. Chem.* **277**, 44332–44338 (2002).

77. Eytan, G. D., Regev, R., Oren, G., Hurwitz, C. D. & Assaraf, Y. G. Efficiency of P-glycoprotein-mediated exclusion of rhodamine dyes from multidrug-resistant cells is determined by their passive transmembrane movement rate. *Eur. J. Biochem.* **248**, 104–112 (1997).

78. Zenaro, E., Piacentino, G. & Constantin, G. The blood-brain barrier in Alzheimer's disease. *Neurobiol. Dis.* **107**, 41–56 (2017).

79. Ulrich, J. D., Huynh, T. P. & Holtzman, D. M. Re-evaluation of the Blood-Brain Barrier in the Presence of Alzheimer's Disease Pathology. *Neuron* **88**, 237–239 (2015).

80. Provias, J. & Jeynes, B. The Role of the Blood-Brain Barrier in the Pathogenesis of Senile Plaques in Alzheimer ' s Disease. *Int. J. Alzheimers. Dis.* **2014**, (2014).

81. Zheng, Q. *et al.* The influence and mechanism of ligustilide , senkyunolide I , and senkyunolide A on echinacoside transport through MDCK - MDR1 cells as blood – brain barrier in vitro model. *Phyther. Res.* 1–10 (2017). doi:10.1002/ptr.5985

82. Hellinger, E. *et al.* Comparison of brain capillary endothelial cell-based and epithelial (MDCK-MDR1, Caco-2, and VB-Caco-2) cell-based surrogate blood-brain barrier penetration models. *Eur. J. Pharm. Biopharm.* **82**, 340–351 (2012).

83. Quan, Y. *et al.* Expression profile of drug and nutrient absorption related genes in Madin-Darby Canine Kidney (MDCK) cells grown under differentiation conditions. *Pharmaceutics* **4**, 314–333 (2012).

84. Lam, K. C. L. & Rajaraman, G. Assessment of P-glycoprotein substrate and inhibition potential of test compounds in MDR1-transfected MDCK cells. *Curr.*

Protoc. Pharmacol. 1–17 (2012). doi:10.1002/0471141755.ph0713s58

85. Pastan, I. *et al.* A retrovirus carrying an MDR1 cDNA confers multidrug resistance and polarized expression of P-glycoprotein in MDCK cells. *Proc. Natl. Acad. Sci.* **85**, 4486–4490 (1988).

86. Wang, Q. *et al.* Evaluation of the MDR-MDCK cell line as a permeability screen for the blood–brain barrier. *Int. J. Pharm.* **288**, 349–359 (2004).

87. Inai, T., Kobayashi, J. & Shibata, Y. Claudin-1 contributes to the epithelial barrier function in MDCK cells. *Eur. J. Cell Biol.* **78**, 849–55 (1999).

88. Schwab, D., Fischer, H., Tabatabaei, A., Poli, S. & Huwyler, J. Comparison of in vitro P-glycoprotein screening assays: Recommendations for their use in drug discovery. *J. Med. Chem.* **46**, 1716–1725 (2003).

89. Feng, B. *et al.* In vitro P-glycoprotein assays to predict the in vivo interactions of P-glycoprotein with drugs in the central nervous system. *Drug Metab. Dispos.* **36**, 268–275 (2008).

90. Lemaire, S., Van Bambeke, F., Mingeot-Leclercq, M. P. & Tulkens, P. M. Modulation of the cellular accumulation and intracellular activity of daptomycin towards phagocytized Staphylococcus aureus by the P-glycoprotein (MDR1) efflux transporter in human THP-1 macrophages and madin-darby canine kidney cells. *Antimicrob. Agents Chemother.* **51**, 2748–2757 (2007).

91. Tang, F., Horie, K. & Borchardt, R. T. Are MDCK cells transfected with the human MDR1 gene a good model of the human intestinal mucosa? *Pharm. Res.* **19**, 765–772 (2002).

92. Taub, M., Podila, L., Ely, D. & Almeida, I. Functional assessment of multiple P-

glycoprotein (P-gp) probe substrates: influence of cell line and modulator concentration on P-gp activity. *Drug Metab. Dispos.* **33**, 1679–1687 (2005).

93. Vogelgesang, S. *et al.* The role of P-glycoprotein in cerebral amyloid angiopathy; implications for the early pathogenesis of Alzheimer's disease. *Curr. Alzheimer Res.* **1**, 121–125 (2004).

94. Vogelgesang, S. *et al.* Implications for the Early Pathogenesis of Alzheimer's Disease. *Curr. Alzheimer Res.* **1**, 121–125 (2009).

95. Cirrito, J. R. *et al.* P-glycoprotein deficiency at the blood-brain barrier increases amyloid-beta deposition in an Alzheimer disease mouse model. *J. Clin. Invest.* **115**, 3285–3290 (2005).

96. Candela, P. *et al.* Apical-to-basolateral transport of amyloid-β peptides through blood-brain barrier cells is mediated by the receptor for advanced glycation end-products and is restricted by p-glycoprotein. *J. Alzheimer's Dis.* **22**, 849–859 (2010).

97. Hartz, A. M. S., Miller, D. S. & Bauer, B. Restoring Blood-Brain Barrier P-Glycoprotein Reduces Brain Amyloid-β in a Mouse Model of Alzheimer's Disease □. *Mol. Pharmacol.* **77**, (2010).

98. Abuznait, A. H., Cain, C., Ingram, D., Burk, D. & Kaddoumi, A. Up-regulation of P-glycoprotein reduces intracellular accumulation of beta amyloid: Investigation of P-glycoprotein as a novel therapeutic target for Alzheimer's disease. *J. Pharm. Pharmacol.* **63**, 1111–1118 (2011).

99. Qosa, H. *et al.* Differences in amyloid-β clearance across mouse and human blood-brain barrier models: Kinetic analysis and mechanistic modeling.

Neuropharmacology **79**, 668–678 (2014).

100. Lam, F. C. *et al.* Beta-Amyloid efflux mediated by p-glycoprotein. *J. Neurochem.* **76**, 1121–1128 (2001).

101. Kuhnke, D. *et al.* MDR1-P-glycoprotein (ABCB1) mediates transport of Alzheimer's amyloid-beta peptides - Implications for the mechanisms of Abeta clearance at the blood-brain barrier. *Brain Pathol.* **17**, 347–353 (2007).

102. Hartz, a. M. S. *et al.* AB 40 Reduces P-Glycoprotein at the Blood-Brain Barrier through the Ubiquitin-Proteasome Pathway. *J. Neurosci.* **36**, 1930–1941 (2016).

103. Lillis, A. P., Van Duyn, L. B., Murphy-Ullrich, J. E. & Strickland, D. K. LDL receptor-related protein 1: unique tissue-specific functions revealed by selective gene knockout studies. *Physiol. Rev.* **88**, 887–918 (2008).

104. Deane, R. *et al.* LRP/amyloid β-peptide interaction mediates differential brain efflux of Aβ isoforms. *Neuron* **43**, 333–344 (2004).

105. Ito, S., Ohtsuki, S. & Terasaki, T. Functional characterization of the brain-to-blood efflux clearance of human amyloid-β peptide (1-40) across the rat blood-brain barrier. *Neurosci. Res.* **56**, 246–252 (2006).

106. Nazer, B., Hong, S. & Selkoe, D. J. LRP promotes endocytosis and degradation, but not transcytosis, of the amyloid-β peptide in a blood-brain barrier in vitro model. *Neurobiol. Dis.* **30**, 94–102 (2008).

107. Shibata, M. *et al.* Clearance of Alzheimer's amyloid-β 1-40 peptide from brain by LDL receptor – related protein-1 at the blood-brain barrier. *J. Clin. Invest.* **106**, 1489–1499 (2000).

108. Deane, R., Wu, Z. & Zlokovic, B. V. RAGE (Yin) versus LRP (Yang) balance

regulates Alzheimer amyloid β-peptide clearance through transport across the blood-brain barrier. *Stroke* **35**, 2628–2631 (2004).

109. Yamasaki, Y. *et al.* Characterization of P-glycoprotein humanized mice generated by chromosome engineering technology: Its utility for prediction of drug distribution to the brain in humans. *Drug Metab. Dispos.* **46**, 1756–1766 (2018).

110. Kusuhara, H. *et al.* P-Glycoprotein mediates the efflux of quinidine across the blood-brain barrier. *J. Pharmacol. Exp. Ther.* **283**, 574–80 (1997).

111. Wang, E. jia, Casciano, C. N., Clement, R. P. & Johnson, W. W. Active transport of fluorescent P-glycoprotein substrates: Evaluation as markers and interaction with inhibitors. *Biochem. Biophys. Res. Commun.* **289**, 580–585 (2001).

112. Chang, C., Bahadduri, P. M., Polli, J. E., Swaan, P. W. & Ekins, S. Rapid identification of P-glycoprotein substrates and inhibitors. *Drug Metab. Dispos.* **34**, 1976–1984 (2006).

113. Okamura, N. *et al.* Digoxin-cyclosporin A interaction: modulation of the multidrug transporter P-glycoprotein in the kidney. *J Pharmacol Exp Ther* **266**, 1614–1619 (1993).

114. Sparreboom, A. *et al.* Limited oral bioavailability and active epithelial excretion of paclitaxel (Taxol) caused by P-glycoprotein in the intestine. *Proc. Natl. Acad. Sci. U. S. A.* **94**, 2031–5 (1997).

115. Tatsuta, T., Naito, M., Oh-hara, T., Sugawara, I. & Tsuruo, T. Functional involvement of P-glycoprotein in blood-brain barrier. *J. Biol. Chem.* **267**, 20383–20391 (1992).

116. Schinkel, A. H. *et al.* Disruption of the mouse mdr1a P-glycoprotein gene leads to

a deficiency in the blood-brain barrier and to increased sensitivity to drugs. *Cell* **77**, 491–502 (1994).

117. Carrano, A. *et al.* Neurobiology of Aging ATP-binding cassette transporters P-glycoprotein and breast cancer related protein are reduced in capillary cerebral amyloid angiopathy. *Neurobiol. Aging* **35**, 565–575 (2014).

118. Brenn, A. *et al.* Beta-Amyloid Downregulates MDR1-P-Glycoprotein (Abcb1) Expression at the Blood-Brain Barrier in Mice. *Int. J. Alzheimers. Dis.* **2011**, 690121 (2011).

119. Park, R., Kook, S.-Y., Park, J.-C. & Mook-Jung, I. Aβ1-42 reduces P-glycoprotein in the blood-brain barrier through RAGE-NF-κB signaling. *Cell Death Dis.* **5**, e1299 (2014).

120. Deo, A. K. *et al.* Activity of P-Glycoprotein, a β-Amyloid Transporter at the Blood-Brain Barrier, Is Compromised in Patients with Mild Alzheimer Disease. *J. Nucl. Med.* **55**, 1106–1111 (2014).

121. Brenn, A. *et al.* Beta-Amyloid Downregulates MDR1-P-glycoprotein Expression at the Blood-Brain Barrier in Mice. *Int. J. Alzheimers. Dis.* **2011**, 1–6 (2011).

122. Worzfeld, T. & Schwaninger, M. Apicobasal polarity of brain endothelial cells. *J. Cereb. Blood Flow Metab.* **36**, 340–362 (2016).

123. Contino, M. *et al.* A Benzopyrane Derivative as a P-glycoprotein Stimulator: A Potential Agent to Decrease Beta-amyloid Accumualtion in Alzheimer's Disease. *Chem Med Chem* **7**, 391–395 (2012).

124. Jain, S., Rathod, V., Prajapati, R., Nandekar, P. P. & Sangamwar, A. T. Pregnane X Receptor and P-glycoprotein : a connexion for Alzheimer's disease

management. *Mol Divers* **18**, 895–909 (2014).